2

Metamaterials and homogenization of composites

The description of a metamaterial as a homogeneous medium involves averaging over the fluctuations of the electromagnetic fields at two levels. As explained in Section 1.3, the macroscopic Maxwell equations are obtained by averaging the rapidly fluctuating electromagnetic fields at atomic or molecular lengthscales over volumes that contain enough number of polarizable or magnetizable atoms/molecules. Within this framework, susceptibilities for bulk materials can be defined. In the case of metamaterials, the structural units of the metamaterial (see Chapter 3) are assumed to be sufficiently large on a molecular scale so that they can confidently be described by their bulk dielectric permittivity and magnetic permeability, and yet sufficiently small compared with the lengthscales over which the applied fields vary (typically a wavelength). Hence, only the fields due to the first few multipoles of the charge and current distributions induced in the structures contribute to the macroscopic polarization over lengthscales large compared to the metamaterial units. In other words, the fine structure of the charge and current distributions over the structural units is not discernible, but only a few averages such as the corresponding dipolar fields or (rarely) the quadrupolar fields can be resolved through the macroscopic polarization and magnetization. These average quantities determine the effective dielectric permittivity and the magnetic permeability tensors of the *bulk metamaterial*.

The metamaterials this book is devoted to are usually composed of metallic rods, sheets, and rings, usually but not necessarily organized in a periodic fashion. When it can be defined, a unit cell of such metamaterial is typically smaller than the exciting electromagnetic wavelength λ, usually on the order of $\lambda/5$ to $\lambda/10$, but sometimes as small as $\lambda/10000$ as in the case of Swiss roll metamaterial (see Chapter 3). The homogenization question thus arises naturally: inasmuch as dielectric materials composed of atoms can be characterized by an effective dielectric constant at microwave and optical frequencies, do the present metamaterials, discrete in their structure, behave as continuous media in the long wavelength regime? If yes, how large should *large* be before the homogenization approximation breaks down? How do we determine the values of the homogenized parameters? What is their range of validity?

More specifically to the realm of metamaterials, the question is posed in the

following terms: given a medium of rings and rods occupying a certain region of space and given an incident electromagnetic radiation, can we find an effective medium within some spatial boundaries (to be determined) that presents the same scattered fields as the original medium? In addition, in order to be a real effective medium, we have to require that the homogenized parameters be independent of the size of the bulk of the metamaterial and independent on the direction of the incident wave, although the effective parameters can be anisotropic and spatially dispersive.

The homogenization analysis is most conveniently carried out on slabs of metamaterials, infinite along the transverse directions ($\hat{x}$ and $\hat{y}$) and finite along the normal ($\hat{z}$) direction, which we assume to be the direction of propagation of the wave. In addition, the criterion for homogenization can be translated into properties of the reflection and transmission coefficients, so that the homogenization procedure can also be rephrased as follows: can we find an equivalent homogeneous slab of effective parameters between two boundaries z_1 and z_2 such that the reflection and transmission coefficients measured from the metamaterial and the homogeneous medium are identical across all frequencies for various slab thicknesses and incident directions? From the microscopic point of view, the criterion is stated as follows: can we replace the metamaterial with a homogeneous medium of specified material parameters so that the fields in the structured metamaterial, when averaged over some reasonable volume, correspond to the fields in the homogeneous medium? These are the questions addressed in the present chapter, from both a physical and mathematical point of view.

2.1 The homogenization hypothesis

Materials composed of small elements are known to respond as continuous media when the operating wavelength is much larger than the individual constituents. A classical example of such materials are natural dielectrics that can be described by a single parameter, the electric permittivity ε. All the negative and positive charges in a dielectric medium are bound to their location by atomic forces and are therefore not free to move like in a conductor. Under the influence of an external electric field, however, these assemblies of negative and positive charges may slightly reorganize, which results in the creation of bound electric dipoles. From a macroscopic point of view, the orientation of these dipoles generates a polarization vector $\mathbf{P}$ that influences the electric flux density $\mathbf{D}$ such as $\mathbf{D} = \varepsilon_0\mathbf{E} + \mathbf{P}$, where $\mathbf{E}$ is the external applied electric field. This allows one to define a general permittivity ε such that $\mathbf{D} = \varepsilon_0\varepsilon\mathbf{E}$, where naturally ε is defined in terms of the polarization vector. Similarly, magnetic media are described by a magnetic permeability μ, and ε and μ represent

the constitutive parameters essential to the macroscopic Maxwell equations. In our case, the metamaterials are composite structures designed to exhibit specific electromagnetic properties at some particular wavelengths that are much larger than the elementary constituents. It is therefore legitimate to look for homogeneous or effective medium parameters, typically an effective permittivity and an effective permeability.

Like in the case of more standard media, these constitutive parameters directly represent the properties of the medium: isotropic metamaterials should be described by scalar constitutive parameters while anisotropic ones should be described by second rank tensors $\bar{\bar{\varepsilon}}$ and $\bar{\bar{\mu}}$, losses induce an imaginary part to these parameters, frequency dispersion yields frequency-dependent parameters, non-locality makes them spatially dispersive (dependent on k), the passive nature of metamaterials forces the imaginary parts to be positive, reciprocity imposes conditions on the tensors, etc.

The homogenization procedure therefore involves two steps:

1. A hypothesis, more or less refined, on the characteristics of the medium (isotropic vs. anisotropic, lossless vs. lossy, etc). Paradoxically, the properties of the metamaterial are initially unknown, and yet a model has to be chosen to perform the homogenization procedure. Therefore, the model should also be tested *a posteriori*.

2. The determination (or retrieval) of the corresponding constitutive parameters, in their tensorial form in the most general case, using numerical or analytical algorithms.

The first aspect is as important as the second and should not be overlooked, since no matter how elaborate the retrieval algorithm, it is going to be bound by the initial assumptions. For example, various algorithms have been proposed to retrieve scalar ε and μ for metamaterials, but this does not imply that the metamaterial under study is actually isotropic. This only reflects the nature of the assumption: that the metamaterial is *supposed to be* isotropic and that one is interested in retrieving scalar constitutive relations. If, however, the metamaterial is in reality anisotropic, mapping the constitutive tensors onto scalar parameters can induce various artifacts that do not represent the physical reality. Hence, before drawing physical conclusions from retrieved parameters, one must be sure that the *a priori* model is valid. Various physical arguments can be used to that effect.

Once the overall model has been ascertained, the next step is to obviously determine the numerical values of the components of the permittivity and permeability tensors. The number of unknowns is directly related to the model chosen and dictates the number of equations that must be obtained from measurements (either experimental measurements or numerical simulations). For example, a simple lossy isotropic dielectric material exhibits two unknowns, the real and imaginary parts of the scalar permittivity, which can

be obtained from one complex measurement such as the reflection and/or the transmission coefficients. The case presented by metamaterials is slightly more complex since these media are known to have a non-unity magnetic permeability, thus requiring more measurements. In addition, the permittivity and the permeability are frequency dispersive, and hence need to be determined at each frequency.

We should also note that there are more mathematically rigorous homogenization theories that analyze the fields as an asymptotic expansion in terms of the microscopic lengthscale associated with the inhomogeneities. Two scales characterize the variation of the fields inside a metamaterial: one, macroscopic, describes the fields over the bulk metamaterial, while a second one, microscopic, describes the fields over small lengthscales inside a unit. The electromagnetic fields can be written as $E(x, y)$ where the fields have a slow variation with the variable x representing the changing in the fields from unit to unit, and a fast variation with the variable y which represents the variation within the units. The fast variable can be taken to be $y = x/\xi$ where $\xi = a/\lambda$, the ratio of the unit cell size to the wavelength of radiation. The principle of the asymptotic expansion is to expand the field in a series involving powers of the fast variable and retain only the leading order terms in the limit of $\xi \to 0$. A rigorous demonstration of this method is out of the scope of this book and we refer the interested reader to Milton (2002) for an excellent treatment of this topic.

Two methods can usually be employed in order to retrieve the constitutive parameters. The first one is based on a set of measurements of the external emergent quantities, *viz.* the frequency-dependent reflection and transmission coefficients (the total number of measurements depends on how much information is needed to unambiguously determine all the unknowns in the problem). Note that these quantities are typically measured in experiments. This is the method that has been used historically for the retrieval of the permittivity of standard dielectrics, and needs to be slightly revisited in the case of metamaterials. We devote the next couple of sections to this topic. The second method for the retrieval of the constitutive parameters is based on the knowledge of the electromagnetic fields inside the metamaterial, i.e., the internal fields. This method is thus better suited for numerical simulations as the internal fields are not easily experimentally accessible, but some experimental approaches to measure these fields have been proposed as well. More details are given in Section 2.5.

2.2 Limitations and consistency conditions

Before detailing the homogenization procedures per se, it is necessary to say a few words about the limitations of homogenization. As a matter of fact, like we have previously outlined, executing an algorithm and obtaining numerical values for, say, a scalar permittivity and permeability does not represent a proof of homogenization (the algorithm is indeed *designed* to output numerical values, and would do so as soon as it is given some inputs, even if these inputs do not have a physical justification). Although we are interested in homogenizing metamaterials, the range of applicability of such process must be carefully examined. In particular, homogenization would not be valid under the following conditions:

1. When the constituents are not much smaller than the operating wavelength. This includes metamaterials with unit cells large or comparable to the wavelength of radiation, as well as photonic crystals.* In this case, the periodicity of the structure (if it exists) may become an important factor that affects the retrieved values of the permittivity and permeability.

2. When the wave propagation inside the material cannot be described by a single propagating mode. Such situation occurs for example close to the resonance of some constituents of the metamaterials, in photonic crystals when multiple Bragg diffraction modes need to be included, or simply in multi-mode waveguides.

Failing to comply with these conditions may produce unphysical artifacts in the frequency-dependent retrieved parameters, the most common of which are an anti-resonance of the permittivity (with an associated negative imaginary part) at the location of the resonance of the permeability, and possibly a truncated resonance of the index of refraction as pointed out in Koschny et al. (2005). These artifacts have been suggested to be due to the fact that the periodicity of the medium becomes visible at the corresponding frequencies, making the homogenization hypothesis less accurate. A conservative ratio of about 30 between the wavelength and the size of the unit cell has been proposed for the homogenization hypothesis to be very well justified, although most of the metamaterials realized to date exhibit a ratio of about 10 at best.

Additionally, an important test of homogenization is to verify that different methods yield comparable values for the effective medium parameters. This is

*More details on photonic crystals are provided in Chapter 4. For the purpose of the present discussion, it is enough to know that photonic crystals are dielectric structures exhibiting a periodicity close to half wavelength, and thus operate in a Bragg diffraction regime.

particularly true for comparison between those methods that utilize the external emergent quantities and those methods that use the internal fields. Note also that the retrieved effective medium parameters should be independent of the particular location of the volume over which the fields are averaged. Equivalently, in methods where the reflection and transmission coefficients are utilized, the retrieved effective medium parameters should be independent of the angle of incidence. In many metamaterials, when the structures are not substantially smaller than the wavelength of light, these conditions can be violated. One should note that even in these cases, it might be possible to define more restricted *equivalent medium parameters* that are specific to a set of angles of incidence and so on. However, the *equivalent medium parameters* cannot be consistently used for the calculations of other properties such as the rate of dissipation in the medium or the scattering property of another object embedded in the metamaterial. An example of such a restricted effective medium theory are the extensions of the Maxwell-Garnett theory based on the Mie scattering coefficients discussed in Section 2.5.2.

Finally, it has been argued (Belov et al. 2003) that spatial dispersion phenomena may occur in some lattice-based structures and should be incorporated in the effective medium model. This non-locality of the constitutive relations, usually apparent in the small wavelength limit, has been found in the large wavelength limit for a metamaterial composed of a series of parallel conducting wires when the incident wave-vector exhibits a component parallel to the axis of the wires. Although our subsequent in-plane incidences ensure that non-local effects are negligible, it is important to keep this effect in mind and accounted for in the treatment of general oblique incidences on metamaterial structures.

2.3 Forward problem

Once a model for the constitutive parameters has been physically justified, enough information needs to be gathered in order to determine the unknown values that populate the constitutive tensors. Traditionally, one method has been overwhelmingly used, which is based on the measurement of the complex reflection and transmission coefficients. This method is appealing because of its relative simplicity to set up in an experimental configuration, as well as its numerical efficiency since the electromagnetic fields need only to be computed over surfaces instead of volumes. In this procedure, the reflection and transmission coefficients (R and T) are used as the linking information between the incident electromagnetic field and the constitutive parameters, the latter relationship being essentially the purpose of inversion or parameter retrieval algorithms.

2.3.1 Relation between R and T and the electromagnetic fields

The first step is to determine the relationship between the incident, reflected, and transmitted fields and the reflection/transmission coefficients. In order to comply to the previous hypothesis, a medium is supposed to be of infinite extent in the transverse $\hat{x}$ and $\hat{y}$ directions and of finite extent in the propagation direction $\hat{z}$. The single propagating mode here is taken to be a plane wave, equivalent to the TEM mode in a parallel plate waveguide. The incident field propagating in the $-\hat{z}$ direction can therefore be written as

$$\mathbf{E}_{inc}(x,y,z) = \hat{e} E_0 \, e^{\mathrm{i}\mathbf{k}_i \cdot \mathbf{r}} \,, \tag{2.1}$$

where $\hat{e}$ is the polarization of the incident field in the xy plane, $\mathbf{k}_i = \hat{x}k_x + \hat{y}k_y - \hat{z}k_z$ is the incident wave-vector of amplitude k, and $\mathbf{r} = \hat{x}x + \hat{y}y + \hat{z}z$ is the position vector. A homogeneous effective medium is sought between the boundaries $z = z_1$ and $z = z_2$, thus defining an incident and transmitted region. In the incident region, the total electric field at $z = z_1$ is given by

$$\begin{aligned} E_{\mathrm{tot}}(x,y,z_1) &= E_0 \, e^{\mathrm{i}k_x x + \mathrm{i}k_y y} \left[e^{-\mathrm{i}k_z z_1} + R \, E_0 \, e^{\mathrm{i}k_z z_1} \right] \\ &= E_{\mathrm{inc}}(x,y,z_1) + R \, E_0 \, e^{\mathrm{i}k_x x + \mathrm{i}k_y y} \, e^{\mathrm{i}k_z z_1}, \end{aligned} \tag{2.2}$$

where R is the reflection coefficient at the first boundary. From this relation, R is obtained as

$$R = \frac{E_{\mathrm{tot}}(x,y,z_1) - E_{\mathrm{inc}}(x,y,z_1)}{E_0 \, e^{\mathrm{i}k_x x + \mathrm{i}k_y y} \, e^{\mathrm{i}k_z z_1}} = \frac{E_{\mathrm{scat}}(x,y,z_1)}{E_{\mathrm{inc}}(x,y,z_1)} \, e^{-2\mathrm{i}k_z z_1}. \tag{2.3}$$

In the transmitted region, the total field at $z = z_2$ is given by

$$E_{\mathrm{tot}}(x,y,z_2) = T \, E_0 \, e^{\mathrm{i}k_x x + \mathrm{i}k_y y} \, e^{-\mathrm{i}k_z z_2}, \tag{2.4}$$

where T is the transmission coefficient given by

$$T = \frac{E_{\mathrm{tot}}(x,y,z_2)}{E_{\mathrm{inc}}(x,y,z_2)} \,. \tag{2.5}$$

Consequently, once the incident and total electric fields are known at $z = z_1$ and $z = z_2$ (either from measurements or numerical simulations), the reflection and transmission coefficients are completely specified.

2.3.2 Determining the electromagnetic fields

A typical configuration is illustrated in Fig. 2.1 for the particular case of a periodic medium: Fig. 2.1(a) shows a material composed of a succession of unit cells that are much smaller than the wavelength (the elements are for the moment supposed to be non-resonant), while Fig. 2.1(b) shows the

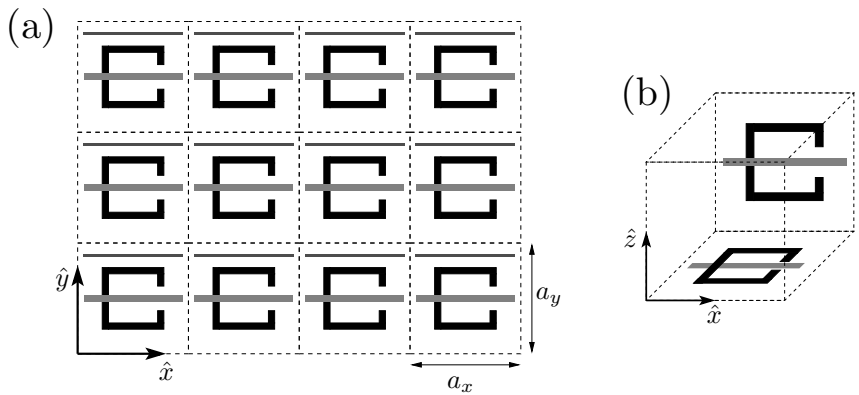

(a) A composite medium assumed to be of infinite extent along the $\hat{x}$ and $\hat{y}$ directions.

(b) A unit cell of the composite medium.

Figure 2.1 Schematic illustration of a periodic medium composed of split rings and rods.

details of a unit cell in three dimensions. In practice, the material should contain many unit cells (the overall size of the material should be of a few wavelengths), while in simulation, the assumption of an infinite medium in the lateral directions ($\hat{x}$ and $\hat{y}$ in our case) is often excellent and considerably reduces the computational requirements. Hence, Fig. 2.1(b) illustrates a unit cell that needs to be analyzed with the proper boundary conditions along the $\hat{x}$ and $\hat{y}$ directions. The material is of finite extent in the $\hat{z}$ direction, which is the principal direction of propagation of the electromagnetic radiation.

The computation of the reflection and transmission coefficients in Eqs. (2.3) −(2.5) requires the knowledge of the scattered electromagnetic fields. Various numerical algorithms are available toward this end, some of the most common ones being the Finite-Difference Time-Domain Method (FDTD), Finite Element Method (FEM), the Transfer Matrix Method, or an integral equation method such as the Method of Moments. The first three methods have the appeal of an extreme generality and mathematical simplicity: they have been applied for many years to solve a plethora of electromagnetic problems, and are well documented in various references. We shall therefore not contribute to an additional description of these methods but refer the reader to references such as Silvester and Ferrari (1996), Taflove and Hagness (2005). The integral equation approach, on the other hand, is usually less commented so that we provide subsequently some details on how to apply it to periodic metamaterials composed of metallic elements. The expert, the uninitiated reader or a reader not interested in the details of the method can therefore skip to the last paragraph of this section.

The integral equation approach is typically mathematically more involved

than methods such as the FDTD or the FEM, but often results in reduced computational times because most of the structure's complexity can be embedded in the kernel of the method, the Green's function. Eqs. (2.3) and (2.5) indicate that it is necessary to know the electric field at various locations in order to compute the reflection and transmission coefficients. The electric field is obtained from the electric sources (magnetic sources can be added by duality) as

$$\mathbf{E}(\mathbf{r}) = \mathrm{i}\omega\mu \iiint \mathrm{d}\mathbf{r}' \, \bar{\bar{G}}(\mathbf{r}, \mathbf{r}') \cdot \mathbf{J}(\mathbf{r}'), \tag{2.6}$$

where $\mathbf{r}$ denotes the observation position while $\mathbf{r}'$ denotes the source position, $\bar{\bar{G}}$ is the dyadic Green's function and $\mathbf{J}$ represents the current sources that can be expressed in a similar manner as the electric field:

$$\mathbf{J}(\mathbf{r}) = \iiint \mathrm{d}\mathbf{r}' \, \delta(\mathbf{r} - \mathbf{r}') \, \mathbf{J}(\mathbf{r}'). \tag{2.7}$$

The triple integral in Eq. (2.6) is defined over the primed coordinates, i.e., over the volume where the sources are defined. In the case of metamaterials for example, the sources are typically surface currents induced on metallic structures (the geometrical units composing typical metamaterials are presented in detail in Chapter 3), so that the three-fold integral reduces to a two-fold integral over the surface of the metallizations.

Combining these equations with the vectorial wave equation for the electric field yields

$$\nabla \times \nabla \times \mathbf{E}(\mathbf{r}) - k^2 \mathbf{E}(\mathbf{r}) = \mathrm{i}\omega\mu \mathbf{J}(\mathbf{r}), \tag{2.8}$$

where k is the wavenumber. It can be directly shown that the Green's function satisfies the relation (Tai 1993)

$$\nabla \times \nabla \times \bar{\bar{G}}(\mathbf{r}, \mathbf{r}') - k^2 \bar{\bar{G}}(\mathbf{r}, \mathbf{r}') = \bar{\bar{I}} \delta(\mathbf{r} - \mathbf{r}'). \tag{2.9}$$

Finally, the dyadic Green's function itself can be expressed in terms of a scalar Green's function $g(\mathbf{r}, \mathbf{r}')$ as

$$\bar{\bar{G}}(\mathbf{r}, \mathbf{r}') = \left(\bar{\bar{\mathrm{I}}} + \frac{1}{k^2} \nabla\nabla \right) g(\mathbf{r}, \mathbf{r}') \, . \tag{2.10}$$

The problem of computing the electric field is therefore reduced to the problem of finding the scalar Green's function g and walking the previous equations backward: from g determining $\bar{\bar{G}}$ using Eq. (2.10), and subsequently determining the electric field $\mathbf{E}$ using Eq. (2.6) knowing the sources in the problem. This last step is usually not straightforward and requires the use of a numerical method such as the Method of Moments (Harrington 1993). In the case of a free-space background, the scalar Green's function is simply given by

$$g(\mathbf{r}, \mathbf{r}') = \frac{e^{\mathrm{i}k|\mathbf{r} - \mathbf{r}'|}}{4\pi|\mathbf{r} - \mathbf{r}'|} \, . \tag{2.11}$$

The appeal of an integral equation-based approach is to reduce the numerical burden (typically to solve Eq. (2.6) like already mentioned) by incorporating as much information analytically into the Green's function as possible. In the case of a periodic metamaterial for example, the periodicity can be incorporated into the expression of g, thus enabling the numerical method to be applied only to a unit cell rather than to the entire structure (note that a similar technique can be applied within the FDTD or FEM, upon applying the proper boundary conditions at the edges of the unit cell). Upon defining a_x and a_y to be the dimensions of the unit cell in the $\hat{x}$ and $\hat{y}$ directions, respectively, the periodic scalar Green's function is immediately obtained from the Bloch theorem as

$$g(\mathbf{r}'') = \sum_{n_1,n_2} \exp(\mathrm{i}\mathbf{k}\cdot\mathbf{R}) \frac{e^{\mathrm{i}k_0|\mathbf{r}''-\mathbf{R}|}}{4\pi|\mathbf{r}''-\mathbf{R}|}\,, \tag{2.12}$$

where $\mathbf{r}'' = \mathbf{r} - \mathbf{r}'$ and

$$\mathbf{R} = n_1\mathbf{a}_x + n_2\mathbf{a}_y \tag{2.13}$$

is a vector of the lattice, n_1 and n_2 being two integers. In the case of a square lattice for example, $\mathbf{a}_x = \hat{x}a_x$, $\mathbf{a}_y = \hat{y}a_y$, and the Green's function is written as

$$g(x'', y'', z'') \sum_{n_1,n_2} e^{\mathrm{i}(k_x n_1 a_x + k_y n_2 a_y)} \frac{e^{\mathrm{i}k_0 R_{n_1 n_2}}}{4\pi R_{n_1 n_2}}\,, \tag{2.14a}$$

where $x'' = x - x'$, $y'' = y - y'$, $z'' = z - z'$ and where

$$\begin{aligned} R_{n_1 n_2} &= \sqrt{(x - x' - n_1 a_x)^2 + (y - y' - n_2 a_y)^2 + (z - z')^2} \\ &= \sqrt{s(1)^2 + s(2)^2 + s(3)^2}\,. \end{aligned} \tag{2.14b}$$

For numerical purposes, the sum in Eq. (2.14a) is truncated at an upper limit N_s which needs to be determined from convergence considerations. These considerations reveal that Eq. (2.14a) is slowly convergent, making it somewhat inefficient to calculate the Green's function (Tsang et al. 2000b). An alternative approach is to convert Eq. (2.14a) into the spectral domain. Upon doing so, the expression becomes

$$g(x'', y'', z'') = \frac{\mathrm{i}}{2\Omega} \sum_{l_1,l_2} \frac{1}{k_{z l_1 l_2}} e^{\,i\left[\left(k_x + \frac{2\pi l_1}{a_x}\right)x'' + \left(k_y + \frac{2\pi l_2}{a_y}\right)y''\right]} e^{\mathrm{i}k_{z l_1 l_2}|z''|}\,, \tag{2.15a}$$

where

$$k_{z l_1 l_2} = \sqrt{k_0^2 - \left(k_x + \frac{2\pi l_1}{a_x}\right)^2 - \left(k_y + \frac{2\pi l_2}{a_y}\right)^2} \tag{2.15b}$$

with $\mathrm{Im}\{k_{z l_1 l_2}\} > 0$ and $\Omega = a_x\, a_y$ is the surface of a periodic unit. The numerical evaluation of this expression shows already a much faster convergence rate than Eq. (2.14a). This rate of convergence can still be increased by using

a method proposed by Ewald (Ewald 1921). The latter starts by splitting the scalar Green's function into two components:

$$g(x'', y'', z'') = g_1(x'', y'', z'') + g_2(x'', y'', z'')\,, \tag{2.16a}$$

where

$$g_1(x'', y'', z'') = \frac{\mathrm{i}}{4\Omega} \sum_{l_1=-N_1}^{N_1} \sum_{l_2=-N_1}^{N_1} \frac{1}{k_{z l_1 l_2}}\, e^{i\,[(k_x + \frac{2\pi l_1}{a_x})\,x'' + (k_y + \frac{2\pi l_2}{a_y})\,y'']} \left\{ e^{\mathrm{i}k_{z l_1 l_2} z''} \mathrm{erfc}(-\frac{\mathrm{i}k_{z l_1 l_2}}{2\,E} - Ez'') + e^{-\mathrm{i}k_{z l_1 l_2} z''} \mathrm{erfc}(-\frac{\mathrm{i}k_{z l_1 l_2}}{2\,E} + Ez'') \right\}, \tag{2.16b}$$

$$g_2(x'', y'', z'') = \sum_{n_1=-N_2}^{N_2} \sum_{n_2=-N_2}^{N_2} \frac{1}{8\pi R_{n_1 n_2}}\, e^{\mathrm{i}(k_x n_1 a_x + k_y n_2 a_y)}\,, \left\{ e^{\mathrm{i}k_0 R_{n_1 n_2}} \mathrm{erfc}(R_{n_1 n_2} E + \frac{\mathrm{i}k_0}{2E}) + e^{-\mathrm{i}k_0 R_{n_1 n_2}} \mathrm{erfc}(R_{n_1 n_2} E - \frac{\mathrm{i}k_0}{2E}) \right\}, \tag{2.16c}$$

where E is Ewald's parameter chosen as $E = \sqrt{\pi/\Omega}$ (Tsang et al. 2000b).

The expression of both g_1 and g_2 can be simplified if the parameter $k_{z l_1 l_2}$ is real (for g_1) and if k_0 is real (for g_2). The simplifications use the properties of the error and complementary error functions:

$$\mathrm{erf}(a + \mathrm{i}b) \doteqdot A + \mathrm{i}B \qquad \mathrm{erfc}(a + \mathrm{i}b) = 1 - A - \mathrm{i}B \doteqdot C + \mathrm{i}D \tag{2.17a}$$

$$\mathrm{erf}(a - \mathrm{i}b) = A - \mathrm{i}B \qquad \mathrm{erfc}(a - \mathrm{i}b) = 1 - A + \mathrm{i}B = C - \mathrm{i}D \tag{2.17b}$$

$$\mathrm{erf}(-a + \mathrm{i}b) = -A + \mathrm{i}B \quad \mathrm{erfc}(-a + \mathrm{i}b) = 1 + A - \mathrm{i}B = (2 - C) + \mathrm{i}D \tag{2.17c}$$

In this case:

- If $k_{z l_1 l_2}$ is real:

$$\begin{aligned} &e^{\mathrm{i}k_{z l_1 l_2} z''} \mathrm{erfc}\Big(-\frac{\mathrm{i}k_{z l_1 l_2}}{2\,E} - Ez''\Big) + e^{-\mathrm{i}k_{z l_1 l_2} z''} \mathrm{erfc}\Big(-\frac{\mathrm{i}k_{z l_1 l_2}}{2\,E} + Ez''\Big) \\ &\quad = e^{\mathrm{i}k_{z l_1 l_2} z''} + e^{-\mathrm{i}k_{z l_1 l_2} z''} + 2\mathrm{i}\mathrm{Im} e^{\mathrm{i}k_{z l_1 l_2} z''} \mathrm{erf}\Big(Ez'' + \frac{\mathrm{i}k_{z l_1 l_2}}{2\,E}\Big) \\ &\quad = 2e^{\mathrm{i}k_{z l_1 l_2} z''} - 2\mathrm{i}\mathrm{Im} e^{\mathrm{i}k_{z l_1 l_2} z''} \mathrm{erfc}\Big(Ez'' + \frac{\mathrm{i}k_{z l_1 l_2}}{2\,E}\Big)\,. \end{aligned} \tag{2.18a}$$

- If k_0 is real (i.e., when the background is lossless):

$$\begin{aligned} &e^{\mathrm{i}k_0 R_{n_1 n_2}} \mathrm{erfc}\Big(R_{n_1 n_2} E + \frac{\mathrm{i}k_0}{2E}\Big) + e^{-\mathrm{i}k_0 R_{n_1 n_2}} \mathrm{erfc}\Big(R_{n_1 n_2} E - \frac{\mathrm{i}k_0}{2E}\Big) \\ &\qquad = 2\mathrm{Re} e^{\mathrm{i}k_0 R_{n_1 n_2}} \mathrm{erfc}\Big(R_{n_1 n_2} E + \frac{\mathrm{i}k_0}{2E}\Big)\,. \end{aligned} \tag{2.19}$$

Once the scalar Green's function is determined, the tensorial form of the Green's function needs to be evaluated from Eq. (2.10). Subsequently, we detail this procedure for the Ewald method only since it is the one that is the computationally most effective.

We shall first define $\tilde{g}_1$ as

$$\tilde{g}_1 = e^{\mathrm{i}k_x x'' + \mathrm{i}k_y y''} \left[e^{\mathrm{i}k_{z l_1 l_2} z''} \operatorname{erfc}\left(-\frac{\mathrm{i}k_{z l_1 l_2}}{2E} - E z'' \right) + e^{-\mathrm{i}k_{z l_1 l_2} z''} \operatorname{erfc}\left(-\frac{\mathrm{i}k_{z l_1 l_2}}{2E} + E z'' \right) \right], \tag{2.20}$$

where $k_x = k_{ix} + 2\pi l_1/a_x$ and $k_y = k_{iy} + 2\pi l_2/a_y$. Then

$$\frac{\partial \tilde{g}_1}{\partial x} = \mathrm{i}k_x \tilde{g}_1 \tag{2.21}$$

$$\frac{\partial \tilde{g}_1}{\partial y} = \mathrm{i}k_y \tilde{g}_1 \tag{2.22}$$

$$\frac{\partial \tilde{g}_1}{\partial z} = \mathrm{i}k_z e^{\mathrm{i}k_x x + \mathrm{i}k_y y} \left[e^{\mathrm{i}k_{z l_1 l_2} z} \operatorname{erfc}(-\frac{\mathrm{i}k_{z l_1 l_2}}{2E} - E z'') - e^{-\mathrm{i}k_{z l_1 l_2} z} \operatorname{erfc}(-\frac{\mathrm{i}k_{z l_1 l_2}}{2E} + E z'') \right] \tag{2.23}$$

$$\nabla \frac{\partial \tilde{g}_1}{\partial x} = -\hat{x}\, k_x^2\, \tilde{g}_1 \; - \hat{y}\, k_x k_y\, \tilde{g}_1 \; + \mathrm{i}\hat{z}\, k_x\, \frac{\partial \tilde{g}_1}{\partial z} \tag{2.24}$$

$$\nabla \frac{\partial \tilde{g}_1}{\partial y} = -\hat{x}\, k_x k_y\, \tilde{g}_1 \; - \hat{y}\, k_y^2\, \tilde{g}_1 \; + \mathrm{i}\hat{z}\, k_y\, \frac{\partial \tilde{g}_1}{\partial z} \tag{2.25}$$

$$\nabla \frac{\partial \tilde{g}_1}{\partial z} = \mathrm{i}\hat{x}\, k_x \frac{\partial \tilde{g}_1}{\partial x} \; + \mathrm{i}\hat{y}\, k_y \frac{\partial \tilde{g}_1}{\partial y} \; + \hat{z}\, \frac{\partial^2 \tilde{g}_1}{\partial z^2}\,, \tag{2.26}$$

where

$$\frac{\partial^2 \tilde{g}_1}{\partial z^2} = -k_z^2\, \tilde{g}_1 + \frac{4\mathrm{i}k_z E}{\sqrt{\pi}}\, e^{\mathrm{i}k_x x + \mathrm{i}k_y y} e^{\frac{k_z^2 - 4E^4 z^2}{4E^2}}\,. \tag{2.27}$$

From these relations, we obtain

$$\nabla\nabla \tilde{g}_1 = \begin{pmatrix} -k_x^2 \tilde{g}_1 & -k_x k_y \tilde{g}_1 & \mathrm{i}k_x \frac{\partial \tilde{g}_1}{\partial z} \\ -k_x k_y \tilde{g}_1 & -k_y^2 \tilde{g}_1 & \mathrm{i}k_y \frac{\partial \tilde{g}_1}{\partial z} \\ \mathrm{i}k_x \frac{\partial \tilde{g}_1}{\partial z} & \mathrm{i}k_y \frac{\partial \tilde{g}_1}{\partial z} & \frac{\partial^2 \tilde{g}_1}{\partial z^2} \end{pmatrix} \tag{2.28}$$

and finally

$$\left(\bar{\bar{\mathrm{I}}} + \frac{1}{k^2} \nabla\nabla \right) g_1(\mathbf{r}, \mathbf{r}') \; = \frac{\mathrm{i}}{4\Omega} \sum_{l_1, l_2} \frac{1}{k_{z l_1 l_2}} \left(\bar{\bar{\mathrm{I}}} + \frac{1}{k_0^2} \nabla\nabla \right) \tilde{g}_1\,. \tag{2.29}$$

Next, we define

$$\tilde{g}_2 = \frac{e^{\mathrm{i}k_0 R_{n_1 n_2}}}{R_{n_1 n_2}} \operatorname{erfc}(R_{n_1 n_2} E + \frac{\mathrm{i}k_0}{2E}) + \frac{e^{-\mathrm{i}k_0 R_{n_1 n_2}}}{R_{n_1 n_2}} \operatorname{erfc}(R_{n_1 n_2} E - \frac{\mathrm{i}k_0}{2E})\,, \tag{2.30}$$

where $R_{n_1 n_2}$ has been defined in Eq. (2.14b). Then

$$\frac{\partial \tilde{g}_2}{\partial s_i} = \frac{\partial R_{n_1 n_2}}{\partial s_i}\, \delta \tilde{g}_2\,, \tag{2.31a}$$

$$\frac{\partial}{\partial s_j}\frac{\partial \tilde{g}_2}{\partial s_i} \frac{\partial^2 R_{n_1 n_2}}{\partial s_j \partial s_i}\, \delta \tilde{g}_2 + \frac{\partial R_{n_1 n_2}}{\partial s_j}\, \frac{\partial R_{n_1 n_2}}{\partial s_i}\, \delta^2 \tilde{g}_2\,, \tag{2.31b}$$

where $s_i \in \{x, y, z\}$, $s_j \in \{x, y, z\}$, and

$$\begin{aligned}\delta \tilde{g}_2 - \Bigg[& \frac{4E}{\sqrt{\pi} R_{n_1 n_2}}\, e^{\frac{k_0^2 - 4R_{n_1 n_2}^2 E^4}{4E^2}} \\ & + \frac{1 - \mathrm{i}k_0 R_{n_1 n_2}}{R_{n_1 n_2}}\, \frac{e^{\mathrm{i}k_0 R_{n_1 n_2}}}{R_{n_1 n_2}}\, \operatorname{erfc}(R_{n_1 n_2} E + \frac{\mathrm{i}k_0}{2E}) \\ & + \frac{1 + \mathrm{i}k_0 R_{n_1 n_2}}{R_{n_1 n_2}}\, \frac{e^{-\mathrm{i}k_0 R_{n_1 n_2}}}{R_{n_1 n_2}}\, \operatorname{erfc}(R_{n_1 n_2} E - \frac{\mathrm{i}k_0}{2E}) \Bigg]\,, \end{aligned} \tag{2.32}$$

$$\begin{aligned}\delta^2 \tilde{g}_2 & \frac{8E}{\sqrt{\pi} R_{n_1 n_2}^2}\, (1 + R_{n_1 n_2}^2 E^2)\, e^{\frac{k^2 - 4R_{n_1 n_2}^2 E^4}{4E^2}} \\ & + \frac{2(1 - \mathrm{i}k_0 R_{n_1 n_2}) - k_0^2 R_{n_1 n_2}^2}{R_{n_1 n_2}^2}\, \frac{e^{\mathrm{i}k_0 R_{n_1 n_2}}}{R_{n_1 n_2}}\, \operatorname{erfc}(R_{n_1 n_2} E + \frac{\mathrm{i}k_0}{2E}) \\ & + \frac{2(1 + \mathrm{i}k_0 R_{n_1 n_2}) - k_0^2 R_{n_1 n_2}^2}{R_{n_1 n_2}^2}\, \frac{e^{-\mathrm{i}k_0 R_{n_1 n_2}}}{R_{n_1 n_2}}\, \operatorname{erfc}(R_{n_1 n_2} E - \frac{\mathrm{i}k_0}{2E})\,. \end{aligned} \tag{2.33}$$

In addition

$$\frac{\partial R_{n_1 n_2}}{\partial s_i} = \frac{s(i)}{R_{n_1 n_2}}\,, \tag{2.34a}$$

$$\frac{\partial^2 R_{n_1 n_2}}{\partial s_i^2} = \frac{R_{n_1 n_2}^2 - s(i)^2}{R_{n_1 n_2}^3}\,, \tag{2.34b}$$

$$\frac{\partial^2 R_{n_1 n_2}}{\partial s_j \partial s_i} = -\frac{s(j)\, s(i)}{R_{n_1 n_2}^3}\,. \tag{2.34c}$$

The second contribution to the dyadic Green's function is finally expressed as

$$\begin{aligned}\left(\bar{\bar{\mathrm{I}}} + \frac{1}{k^2}\nabla\nabla\right) g_2(\mathbf{r}, \mathbf{r}') \; = \; & \sum_{n_1, n_2} \frac{1}{8\pi R_{n_1 n_2}}\, e^{\mathrm{i}(k_x n_1 a_x + k_y n_2 a_y)} \\ & \Bigg[\bar{\bar{\mathrm{I}}} \tilde{g}_2 + \frac{1}{k_0^2} \begin{pmatrix} \frac{\partial^2 R_{n_1 n_2}}{\partial x^2} & \frac{\partial^2 R_{n_1 n_2}}{\partial y \partial x} & \frac{\partial^2 R_{n_1 n_2}}{\partial z \partial x} \\ \frac{\partial^2 R_{n_1 n_2}}{\partial x \partial y} & \frac{\partial^2 R_{n_1 n_2}}{\partial y^2} & \frac{\partial^2 R_{n_1 n_2}}{\partial z \partial y} \\ \frac{\partial^2 R_{n_1 n_2}}{\partial x \partial z} & \frac{\partial^2 R_{n_1 n_2}}{\partial y \partial z} & \frac{\partial^2 R_{n_1 n_2}}{\partial z^2} \end{pmatrix} \delta \tilde{g}_2 \\ & + \frac{1}{k_0^2} \begin{pmatrix} \frac{\partial R_{n_1 n_2}}{\partial x} \\ \frac{\partial R_{n_1 n_2}}{\partial y} \\ \frac{\partial R_{n_1 n_2}}{\partial z} \end{pmatrix} \begin{pmatrix} \frac{\partial R_{n_1 n_2}}{\partial x} & \frac{\partial R_{n_1 n_2}}{\partial y} & \frac{\partial R_{n_1 n_2}}{\partial z} \end{pmatrix} \delta^2 \tilde{g}_2 \Bigg]\,. \end{aligned} \tag{2.35}$$

The total Green's function is given by the sum of the two dyadic components, individually expressed in Eq. (2.29) and Eq. (2.35), and can directly be used in a Method of Moment algorithm. Such an algorithm, being more specific in its applicability, is usually faster than other numerical methods to obtain the electromagnetic fields, and can therefore be used more efficiently for example in the design and optimization of split-ring metamaterials.

The determination of the reflection and transmission coefficients directly follows Eqs. (2.3) and (2.5), where the fields computed using the Method of Moment are integrated over a unit cell surface. An example of transmission coefficient as function of frequency is shown in Fig. 2.2 for the standard square rings whose dimensions are detailed in the caption of the figure. It is seen that when the metamaterial contains only rings, the transmission exhibits a stop-band around 15 GHz, which corresponds to the center frequency of the negative permeability band. The medium of rods only, not shown here, exhibits a very low transmission in agreement with a Drude model with a plasma frequency of about 27 GHz. Noticeably, when both rings and rods constitute the metamaterial, a pass-band appears at about 15.2 GHz, within the region of negative permeability and negative permittivity where propagating waves are supported, which actually corresponds to a negative index of refraction as discussed in Chapter 3. These conclusions have been confirmed by the retrieval process detailed subsequently.

2.4 Inverse problems: retrieval and constitutive parameters

2.4.1 Standard media

The previous section was concerned with the determination of the electromagnetic fields scattered by a slab of metamaterial structure in order to obtain the reflection and transmission coefficients. This section is devoted to the other aspect of the problem: how to determine the constitutive parameters of an effective medium once the reflection and transmission coefficients are known.

In a numerical or experimental setup, the configuration often looks like the one depicted in Fig. 2.3: the sample of material whose constitutive parameters are unknown is placed inside a parallel-plate waveguide and is illuminated by a TEM incidence. The reflection and transmission coefficients, in form of S parameters, are measured with respect to some reference planes situated at a distance d_1 and d_2 from the sample. The electric field in the three regions

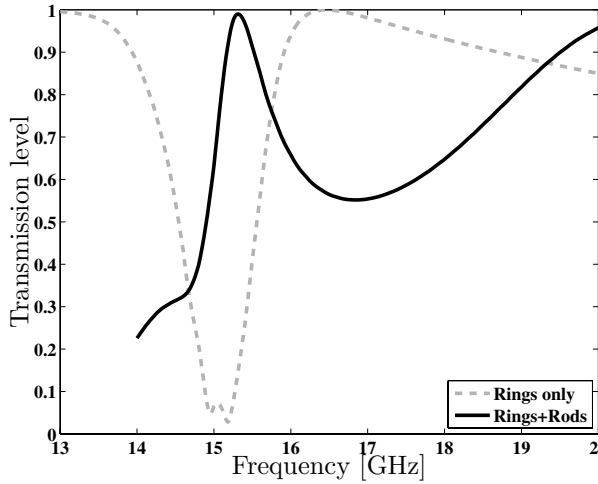

Figure 2.2 Typical transmission curves obtained using the periodic Green's function formalism. The ring-only medium exhibits a stop-band around 15 GHz, whereas the medium of rings+rods exhibits a pass-band at a similar frequency. The rod-only medium, not shown, presents a very low transmission at the frequencies shown (with a plasma frequency of about 27 GHz). The transmission levels have been obtained for a 2-layer metamaterial. The ring is the original square ring shown in Fig. 1.3 of size 3 mm × 3 mm in a lattice of 5 mm × 5 mm, gap and inter-ring spacing of 0.5 mm, and metallization thickness of 0.25 mm. The corresponding rod is centered on the ring, situated 1 mm away from the ring, and with a metallization thickness of 0.5 mm.

thus defined can be written as

$$\mathbf{E}_1 = \hat{y}(e^{\mathrm{i}k_0 z} + C_1 e^{-\mathrm{i}k_0 z}), \tag{2.36a}$$

$$\mathbf{E}_2 = \hat{y}(C_2 e^{\mathrm{i}k_1 z} + C_3 e^{-\mathrm{i}k_1 z}), \tag{2.36b}$$

$$\mathbf{E}_3 = \hat{y}(C_4 e^{\mathrm{i}k_0 z} + C_5 e^{-\mathrm{i}k_0 z}), \tag{2.36c}$$

and it is straightforward to see that $C_5 = 0$.

The coefficients $\{C_i\}$ $(i \in \{1, \ldots, 4\})$ are determined by ensuring the boundary conditions of the tangential electric and magnetic fields at $z = d_1$ and $z = d_1 + d$. The system obtained is

$$\begin{cases} C_1\, e^{-\mathrm{i}k_0 d_1} - C_2\, e^{\mathrm{i}k_1 d_1} - C_3\, e^{-\mathrm{i}k_1 d_1} & = -e^{\mathrm{i}k_0 d_1} \\ \frac{1}{\eta_0} C_1\, e^{-\mathrm{i}k_0 d_1} + \frac{1}{\eta} C_2\, e^{\mathrm{i}k_1 d_1} - \frac{1}{\eta} C_3\, e^{-\mathrm{i}k_1 d_1} & = \frac{1}{\eta_0} e^{\mathrm{i}k_0 d_1} \\ C_2\, e^{\mathrm{i}k_1 (d_1+d)} + C_3\, e^{-\mathrm{i}k_1 (d_1+d)} - C_4\, e^{\mathrm{i}k_0 (d_1+d)} & = 0 \\ -\frac{1}{\eta_1} C_2\, e^{k_1 (d_1+d)} + \frac{1}{\eta_1} C_3\, e^{-k_1 (d_1+d)} + \frac{1}{\eta_0} C_4\, e^{k_0 (d_1+d)} & = 0 \end{cases} \tag{2.37}$$

which contains four equations and four unknowns. The solution is straight-

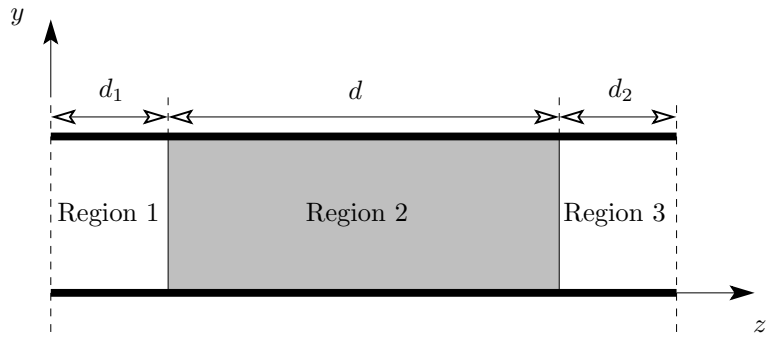

Figure 2.3 Measurement setup in a parallel-plate waveguide: the homogenized medium defines three regions and a reflection/transmission coefficient.

forward and can be written as

$$C_1 = e^{2k_0 d_1}\,\frac{r(1-\Phi^2)}{1-r^2\Phi^2}\,, \tag{2.38a}$$

$$C_2 = e^{-\mathrm{i}d_1(k_1-k_0)}\,\frac{2k_0\mu_1}{(k_1\mu_0+k_0\mu_1)(1-r^2\Phi^2)}\,, \tag{2.38b}$$

$$C_3 = e^{\mathrm{i}d_1(k_1+k_0)}\,\frac{-2k_0\mu_1 r\Phi^2}{(k_1\mu_0+k_0\mu_1)(1-r^2\Phi^2)}\,, \tag{2.38c}$$

$$C_4 = e^{\mathrm{i}d(k_1-k_0)}\,\frac{4k_0\mu_0 k_1\mu}{(k_1\mu_0+k_0\mu_1)^2\,(1-r^2\Phi^2)} = e^{\mathrm{i}d(k_1-k_0)}\,\frac{1-r^2}{1-r^2\Phi^2}\,, \tag{2.38d}$$

where

$$r = \frac{k_0/\mu_0 - k_1/\mu_1}{k_0/\mu_0 + k_1/\mu_1}\,, \tag{2.39a}$$

$$\Phi = \exp(\mathrm{i}k_1 d)\,, \tag{2.39b}$$

r being the reflection coefficient and Φ the phase factor of the transmission coefficient. The S parameters are subsequently defined from Eq. (2.3) and (2.5) as (Nicolson and Ross 1970)

$$S_{11} = \frac{\mathbf{E}_{\mathrm{refl}}(z=0)}{\mathbf{E}_{\mathrm{inc}}(x=0)} = C_1\,, \tag{2.40a}$$

$$S_{21} = \frac{\mathbf{E}_{\mathrm{trans}}(z=d_1+d+d_2)}{\mathbf{E}_{\mathrm{inc}}(z=0)} = C_4\,e^{\mathrm{i}k_0(d_1+d+d_2)}\,. \tag{2.40b}$$

Also, by symmetry, we can compute S_{12} and S_{22} to obtain (Baker-Jarvis et al.

1990)

$$S_{11} = R_1^2 \frac{r(1-\Phi^2)}{1-r^2\Phi^2}\,, \tag{2.41a}$$

$$S_{12} = S_{21} = R_1 R_2 \frac{\Phi(1-r^2)}{1-r^2\Phi^2}\,, \tag{2.41b}$$

$$S_{22} = R_2^2 \frac{r(1-\Phi^2)}{1-r^2\Phi^2}\,, \tag{2.41c}$$

where we have defined

$$R_1 = e^{\mathrm{i}k_0 d_1}\,, \tag{2.42a}$$

$$R_2 = e^{\mathrm{i}k_0 d_2}\,. \tag{2.42b}$$

The problem is therefore reduced to finding a solution to Eqs. (2.41) for r and Φ from the measured S parameters. In these equations, the quantities d_1 and d_2 should also be treated as unknown since the exact distances to the reference planes are often unknown in experimental situations. As a consequence, either for stability or for the number of unknowns, it may appear that Eqs. (2.41) are not sufficient, which prompted Baker-Jarvis et al. (1990) to suggest additional measurements, using the equations depending on what quantities are known to a better precision. The simplest example is of course to invert Φ from its definition in Eq. (2.39b) to obtain

$$\Phi = e^{\mathrm{i}k_1 d} \implies k_1 d = -\mathrm{i}\ln(\Phi) + 2\mathrm{m}\pi\,, \tag{2.43}$$

where m is a positive or negative integer. Once k_1 is known, the permeability is obtained from Eq. (2.39a) as

$$\mu_1 = \mu_0 \frac{k_1}{k_0} \frac{1+r}{1-r} \tag{2.44}$$

and the permittivity is obtained from the k_1 coefficient and the dispersion relation. Note that the choice of m is not always straightforward and deserves further attention, as discussed in the subsequent sections.

2.4.2 Left-handed media

The previous retrieval process has been used extensively on standard dielectric media. The same mathematical formalism can of course be applied to the retrieval of isotropic parameters of left-handed media, although some deeper considerations are necessary due to essentially two aspects:

1. The parameters of left-handed media can take negative values, which also requires them to be complex (to reflect the inherent lossy nature of the media). In the retrieval process, one has therefore to be careful that

no physical laws are violated by the retrieved parameters. In fact, it is judicious to use some physical requirements as inputs into the retrieval algorithm in order to converge to a unique and physical solution.

2. The parameters are frequency dispersive and may have very large values close to resonance. On the contrary, the frequency dispersion of standard media within the frequencies of interest is usually slowly varying. Mathematically, this is reflected by the fact that the parameter m in Eq. (2.43) is usually zero or at most one (it is usually possible to pick samples small compared to the effective wavelength), whereas in the case of left-handed media, it might vary much more. The determination of the proper m therefore becomes a key element of the inversion process.

Based on these considerations, we first rewrite the previous expressions of the S parameters as function of the index of refraction n and impedance z of the medium:

$$S_{11} = \frac{R_{01}(1 - e^{2ink_0d})}{1 - R_{01}^2\, e^{2ink_0d}}\,, \tag{2.45a}$$

$$S_{21} = \frac{(1 - R_{01}^2)e^{2ink_0d}}{1 - R_{01}^2\, e^{2ink_0d}}\,, \tag{2.45b}$$

where $R_{01} = (z-1)/(z+1)$. Note that for the moment, we have assumed that $d_1 = 0$ and that the fields are computed at the second boundary. Let us introduce an intermediary step and first invert for the index of refraction n and the impedance z from these equations as (Smith et al. 2002a)

$$z = \pm\sqrt{\frac{(1+S_{11})^2 - S_{21}^2}{(1-S_{11})^2 - S_{21}^2}}, \tag{2.46a}$$

$$e^{ink_0d} = X \pm \mathrm{i}\sqrt{1 - X^2}, \tag{2.46b}$$

where $X = (1 - S_{11}^2 + S_{21}^2)/(2S_{21})$. The advantage of this intermediary step is that the index of refraction and the impedance are physical quantities upon which a series of requirements can be imposed. Typically, the fact that the medium is passive implies that

$$z' \geq 0, \tag{2.47a}$$

$$n'' \geq 0, \tag{2.47b}$$

where the prime denotes the real part and the double prime denotes the imaginary part, and the sign ambiguity in Eq. (2.46) can be lifted. The complexity due to the branch point of the logarithm function remains however, since the index of refraction is obtained from Eq. (2.46b) as

$$n = \frac{1}{k_0 d}\left\{\left[\left(\ln(e^{ink_0d})''\right) + 2\mathrm{m}\pi\right] - \mathrm{i}\left[\ln(e^{ink_0d})\right]'\right\}. \tag{2.48}$$

The practical implementation of these equations for the retrieval of the index of refraction and the impedance is hindered by a few issues that need to be carefully examined:

1. The practical limitation of Eqs. (2.47).
2. The determination of the integer m.
3. The sensitivity of these parameters to noise.
4. The definition of the material boundaries.

1. The index of refraction n and the impedance z can *a priori* be determined from Eqs. (2.46) and the conditions of Eqs. (2.47). However, this method has an important practical limitation: both numerical simulations and experimental measurements introduce perturbations in the S parameters that translate into perturbations on n and z. These perturbations are typically small and can be filtered out unless the parameters themselves are close to zero, in which case a small perturbation can induce an unphysical sign change.

This issue can be resolved by introducing a threshold in the use of Eqs. (2.47): when the absolute value of z' is greater than the threshold, Eq. (2.47a) can be used. Otherwise, the sign of z is determined such that the corresponding index of refraction has a non-negative imaginary part. This condition is equivalent to $|e^{ink_0d}| \leq 1$, where

$$e^{ink_0d} = \frac{S_{21}}{1 - S_{11}\frac{z-1}{z+1}}\,. \tag{2.49}$$

2. The determination of the branch of n' is not a problem proper to left-handed media as can be seen from Eq. (2.43), but nonetheless it is usually not discussed when effective parameters of standard dielectric are retrieved. The reason is that the integer m in the exponential argument of Eq. (2.46b) can be related to the number of wavelengths that propagate inside the slab. By choosing short samples, it is therefore possible to ensure that the sample is smaller than one wavelength, thus automatically selecting m = 0 as solution. Such strategy works well with standard dielectric, where the constitutive parameters are usually reasonably small within the frequencies of interest and where their variations with respect to frequency are small. In the case of left-handed media, however, the parameters might take large absolute values, either at low frequencies for a Drude model or close to resonance for a Lorentz model. Therefore, the small thickness of the sample does not guarantee a sub-wavelength propagation distance due to the possibly large values of the permittivity and the permeability (and hence the effective wavelength inside the medium is small).

The process of determining the correct branch therefore needs to be carefully examined. Let us divide it into two steps. First, the branch at the

initial frequency is determined. The imaginary parts of the permeability and permittivity can be expressed as

$$\mu'' = n'z'' + n''z' \,, \tag{2.50a}$$

$$\varepsilon'' = (n''z' - n'z'')/|z|^2. \tag{2.50b}$$

The requirement of positive imaginary parts for both ε and μ leads to $|n'z''| \leq n''z'$. At low frequencies, n'' is usually close to zero so that $n''z'$ is small. Since z'' may not be small itself, n' should be small and m can be determined such that this condition is true. Upon doing so, either a single solution or multiple solutions can be obtained. In the latter case, each solution should be examined in order to make sure that the condition $|n'z''| \leq n''z'$ is satisfied at all subsequent frequencies as well, which usually only leaves one solution to the problem.

The second step in determining the correct branch is to obtain the parameters at all subsequent frequencies. This can be done by invoking the continuity of the permittivity and the permeability, and implementing an iterative scheme based on the parameters at the first frequency.[†] Assuming continuity with frequency, we can Taylor expand (Chen et al. 2004c)

$$e^{\mathrm{i}n(f_1)k_0(f_1)d} \simeq e^{\mathrm{i}n(f_0)k_0(f_0)d}\left(1 + \Delta + \frac{1}{2}\Delta^2\right), \tag{2.51}$$

where $\Delta = \mathrm{i}n(f_1)k_0(f_1)d - \mathrm{i}n(f_0)k_0(f_0)d$, k_0 is the wave-number in free-space, f_0 is the frequency at which all the parameters are known, and f_1 is the next frequency. Eq. (2.51) is a second-degree polynomial for the unknown $n(f_1)$ where all other terms are known (in particular, the left-hand side is directly obtained from Eq. (2.49)). The selection between the two solutions is performed by comparing $n''(f_1)$ with the value already obtained from Eqs. (2.48) and (2.46b). The closest root is selected as the correct one, whose real part can be used to determine the branch m.

3. The sensitivity to measurements is most prominent in two situations: when the transmission is either close to zero or close to unity. In the first case, which typically appears below the resonance band, $|S_{21}|$ is close to zero which yields large values of the X parameters in Eq. (2.46b) and hence, strong variations in the index of refraction (seen as unphysical spikes in the retrieved values). This situation is avoided by solving first for the impedance. The latter is indeed stable as can be seen by inspecting the first derivative

$$\frac{\partial z^2}{\partial S_{21}} = \frac{8S_{21}S_{11}}{[(1 - S_{11}]^2 - S_{21}^2]}. \tag{2.52}$$

[†]This method should be used cautiously when crossing a resonant region if losses are small. An alternative is to apply the method from low frequencies up to the resonance, and again in a backward fashion from very high frequencies down to the resonance.

The second situation is the mirror of this first one: the impedance is unstable, whereas the index of refraction is stable and should be used first in the retrieval process. Eqs. (2.45) can then be solved within a threshold.

4. The purpose of the homogenization procedure is to find the effective parameters of metamaterials, but also to find the boundaries of the effective medium. The metamaterials being usually composed of discrete metallic elements, it is not immediately clear where these boundaries should be.

The determination of the boundaries can be performed based on the requirement of homogenization, namely that the effective parameters of two slabs of different thicknesses should be identical at all frequencies. This principle, along with the fact that the impedance depends on the slab thickness, can be used to set up a minimization problem: the impedances of two different metamaterial slabs are computed, and their difference is optimized across the entire frequency spectrum of interest as function of the boundaries of the medium. The boundaries that reach the minimum in a pre-defined sense are chosen to be the boundaries of the effective medium.

In the case of periodic structures, this method yields the expected results that the effective boundaries coincide with the boundaries of the unit cell of the metamaterial. In case of non-periodic, or non-symmetric cells (Smith et al. 2005), the optimization might yield different results, which are, of course, dependent on the particular case under study.

A typical retrieval result is shown in Fig. 2.4 (Chen et al. 2004c) for the permittivity and the permeability of a wire-split ring composite metamaterial, for which the four issues aforementioned have been resolved as indicated. Note the good agreement of the permittivity with a Drude model and of the permeability with a Lorentz model, which justifies the effective models used to represent metamaterials. Note also that the region close to the resonance of the permeability, where the retrieval results are not accurate and where unphysical artifacts occur, has not been shown.

2.5 Homogenization from averaging the internal fields

The effective medium parameters such as ε and μ usually relate two fields:

$$\langle \mathbf{D} \rangle = \varepsilon_0 \varepsilon \cdot \langle \mathbf{E} \rangle, \qquad \langle \mathbf{B} \rangle = \mu_0 \mu \cdot \langle \mathbf{H} \rangle, \tag{2.53}$$

where the fields have been averaged over some volume in the medium and where the angular brackets $\langle\ \rangle$ indicate averages taken over some relevant volume. Here $\mathbf{E}$ and $\mathbf{H}$ are the applied electric and magnetic fields. The bulk average polarization or magnetization in the medium is

$$\langle \mathbf{P} \rangle = N \langle \mathbf{p} \rangle \qquad \langle \mathbf{M} \rangle = N \langle \mathbf{m} \rangle \,, \tag{2.54}$$

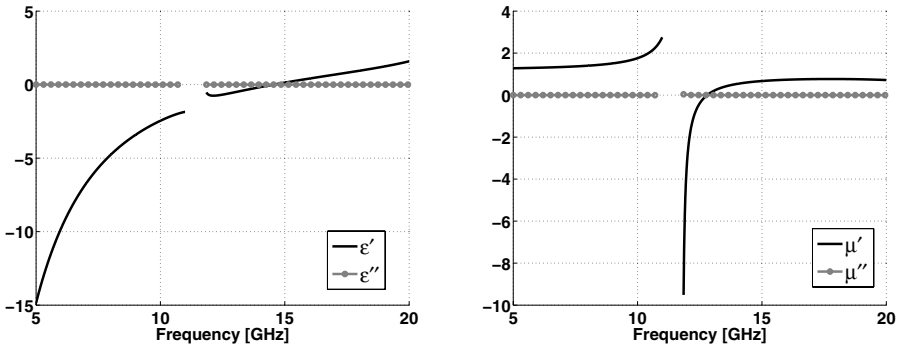

Figure 2.4 Typical retrieval results for the permittivity and the permeability of a split-ring medium (Chen et al. 2004c).

where N is the relevant density of the polarizable or magnetizable structural units, and $\mathbf{p}$ and $\mathbf{m}$ are the electric and magnetic dipole moment that develop in a structural unit. One principal task is therefore to determine the individual polarizabilities or magnetizabilities of the individual structural units, in which analytical and numerical modeling plays an important role. The dipole moments generated in an individual structural unit are related to the total fields at that given point and are not only determined by the applied electromagnetic fields, since the fields due to other induced dipole moments in the medium also affect the dipole moments. While these fields can be neglected if the medium is dilute enough (for small filling factor f), any homogenization procedure would need to also account for these fields. A somewhat elementary correction in this regard was discussed in Section 1.3.2 in calculating the bulk dielectric permittivity of a dense molecular medium (the Clausius-Mossotti relationship).

We subsequently discuss some rather elementary ideas by which one can determine effective medium parameters by carrying out appropriate averages of these fields inside the metamaterial. Again, the physical model of the metamaterial that allows us to make some assumptions about the nature of the electromagnetic fields in the metamaterial is as important as the algorithm that allows us to retrieve values for the effective medium parameters from the knowledge of the fields.

2.5.1 Maxwell-Garnett effective medium theory

The Maxwell-Garnett approach (Maxwell-Garnett 1904) has been a very successful theory in describing the effective dielectric properties of composite dielectric media. The composite medium is assumed to be composed of small particles of radius $r \ll \lambda$ and dielectric permittivity ε_i randomly embedded in another bulk medium with dielectric permittivity ε_h. The volume filling frac-

tion of the included particles is taken to be f. The Maxwell-Garnett approach incorporates the distortions due to the dipole field on an average and has been very successful in describing the properties of dilute random inhomogeneous materials. If f is small, then the particles effectively do not feel the scattered fields of other particles, and one can write the dielectric permittivity for a dilute medium of small spherical particles simply as (Landau et al. 1984)

$$\varepsilon_{\text{eff}} = \varepsilon_h + 3f\varepsilon_h \frac{\varepsilon_i - \varepsilon_h}{\varepsilon_i + 2\varepsilon_h}. \tag{2.55}$$

The second term is immediately recognized to arise from the polarizability of the spherical particles,

$$\alpha = \frac{\varepsilon_i - \varepsilon_h}{\varepsilon_i + 2\varepsilon_h} 4\pi a^3. \tag{2.56}$$

The crucial assumption is that the size parameter of the particle $x = \sqrt{\varepsilon_i} ka \ll 1$ where $k = \omega/c$, which allows the assumption of a spatially uniform field over the entire region of the particle and consequently the use of the static polarizability of the spherical particle.

For a dense concentration of particles, one can carry out a correction to the applied fields to obtain the total fields on the lines of the Lorentz-Lorenz theory (see Section 1.3.2). The effective dielectric permittivity is determined by

$$\frac{\varepsilon_{\text{eff}} - \varepsilon_h}{\varepsilon_{\text{eff}} + 2\varepsilon_h} = \frac{N\alpha}{3}, \tag{2.57}$$

where α is the polarizability of individual particles given above. Hence we can obtain the Maxwell-Garnett effective medium parameter

$$\varepsilon_{\text{eff}} = \varepsilon_h \frac{\varepsilon_i(1+2f) + 2\varepsilon_h(1-f)}{\varepsilon_i(1-f) + \varepsilon_h(2+f)}, \tag{2.58}$$

where the filling $f = 4\pi a^3 N/3$ and n is the number density of the spheres. The effective medium parameter is complex if the dielectric particles have a complex ε. This effective medium theory is an unrestricted theory in that the imaginary part arises from the actual dissipation of energy in the medium. Although the size of the particles does not appear in the final expression for ε, this is only valid when the size $a \ll \lambda$ or ideally for point dipoles.

The Maxwell-Garnett result can be generalized to include corrections for finite size of the particles. Three such extensions have been compared in Ruppin (2000a) and we briefly summarize here only the generalization of Doyle (1989) which was found to be the most successful of the three. This method consists of using the polarizability for the sphere which comes out of a Mie scattering calculation (Bohren and Huffman 1983). The Mie scattering coefficients are given in general by Bohren and Huffman (1983) as

$$a_m = \frac{n\psi_m(nx)\psi'_m(x) - \psi_m(x)\psi'_m(nx)}{n\psi_m(nx)\xi'_m(x) - \xi_m(x)\psi'_m(nx)}, \tag{2.59}$$

$$b_m = \frac{\psi_m(nx)\psi'_m(x) - n\psi_m(x)\psi'_m(nx)}{\psi_m(nx)\xi'_m(x) - n\xi_m(x)\psi'_m(nx)}, \tag{2.60}$$

where $x = ka$ and $n = \sqrt{\varepsilon_i/\varepsilon_h}$ is the relative refractive index of the spheres with respect to the background. Here ψ_m and ξ_m are the Riccati-Bessel functions of order m and related to the spherical Bessel and Hankel's functions as $\psi_m(x) = xj_m(x)$ and $\xi_m(x) = xh_m^{(1)}(x)$ and the primes imply differentiation with respect to the argument. The total extinction cross-section is given by

$$\sigma_{\text{ext}} = \frac{2}{x^2}\sum_{n=1}^{\infty}(2n+1)\ \text{Re}(a_n + b_n). \tag{2.61}$$

The electric dipole moment of the sphere is described by the term a_1, the quadrupole moment by a_2, and so on. The coefficients b_n denote the strengths of the magnetic multipoles. The electric polarizability of the sphere is given by

$$\alpha = \mathrm{i}4\pi a^3 \frac{3a_1}{2x^3}. \tag{2.62}$$

Hence we obtain the effective medium dielectric permittivity as

$$\varepsilon_{\text{eff}} = \varepsilon_h \frac{x^3 + 3\mathrm{i}fa_1}{x^3 - \frac{3}{2}\mathrm{i}fa_1}. \tag{2.63}$$

A similar result can be obtained for the effective magnetic permeability as

$$\mu_{\text{eff}} = \mu_h \frac{x^3 + 3\mathrm{i}fb_1}{x^3 - \frac{3}{2}\mathrm{i}fb_1}. \tag{2.64}$$

It immediately becomes obvious that a system of dielectric particles can have a non-unit effective medium magnetic permeability if the magnetic Mie scattering resonance can contribute effectively as pointed out in Bohren (1986). In fact, this possibility has been effectively used to design magnetic metamaterials as discussed in Section 3.2.5. The extended Maxwell-Garnett theories always yield complex effective medium parameters. In other words, they predict a lossy medium even if the constituent particles or host medium are strictly non-dissipative. The imaginary parts arise due to the scattering phase shifts of the waves. The loss implied does not represent actual absorption of radiation in the medium leading to consequent heating of the medium, but rather represents scattering or radiation losses that are then absorbed by (assumed) absorbers at the boundaries of the medium (at the infinities). Thus, the extended Maxwell-Garnett theories are restricted effective medium theories where the parameters are valid for certain purposes (such as the extinction) while not valid for calculating other properties such as the amount of dissipation. This point has been extensively discussed by Bohren (1986).

2.5.2 Layered media as anisotropic effective media

As another example of a homogenizable medium, let us consider a periodically stratified medium consisting of alternating layers of two media. Let the

dielectric permittivities of the two media be ε_1 and ε_2, and let d_1 and d_2 be the corresponding layer thicknesses. In the limit that the layer thicknesses are extremely small compared to the wavelength of light in the effective medium, one can assume reasonably uniform fields in the layered medium but subject to appropriate boundary conditions. If the electric field is applied parallel to the interfaces, then it is continuous across the layer. Hence we can write

$$E_1 = E_2 = \langle E_\parallel \rangle, \tag{2.65}$$

where E_1 and E_2 are the fields in the two layers. The average displacement field, averaged with respect to the volume fraction, is

$$\langle D_\parallel \rangle = \frac{D_1 d_1 + D_2 d_2}{d_1 + d_2} = \varepsilon_0 \frac{\varepsilon_1 d_1 + \varepsilon_1 d_2}{d_1 + d_2} \langle E_\parallel \rangle, \tag{2.66}$$

which allows us to to define the average relative permittivity in the parallel directions as

$$\varepsilon_\parallel = \frac{\varepsilon_1 + \varepsilon_2 \eta}{1 + \eta}, \tag{2.67}$$

where $\eta = d_2/d_1$. When the applied fields are normal to the interfaces, it is the normal component of the displacement field that is continuous across the layer interfaces. Hence we have

$$D_1 = D_2 = \langle D_\perp \rangle \tag{2.68}$$

and

$$\langle E_\perp \rangle = \frac{E_1 d_1 + E_2 d_2}{d_1 + d_2} = \frac{1}{\varepsilon_0} \frac{\frac{d_1}{\varepsilon_1} + \frac{d2}{\varepsilon_2}}{d_1 + d_2} \langle D_\perp \rangle, \tag{2.69}$$

and we can define the effective permittivity normal to the layers by

$$(\varepsilon_\perp)^{-1} = \frac{\frac{1}{\varepsilon_1} + \frac{\eta}{\varepsilon_2}}{1 + \eta}. \tag{2.70}$$

The layering itself gives rise to an anisotropic response parallel and perpendicular to the layers. The possibility of mixing layers with negative dielectric permittivity (see Section 3.1.1) and positive dielectric permittivity produces an unusual anisotropic dielectric permittivity tensor. Depending on the relative values of ε_1, ε_2, and η, the parallel component can be negative while the perpendicular component can be positive or vice versa. Such anisotropic media are termed *indefinite media* (see Section 5.3.1 on page 202 for a more detailed analysis of indefinite media). As an example, in Fig. 2.5 we plot the effective permittivity components with frequency for a layered medium composed of fused silica and silver (layered along the z-direction). Silver has a negative permittivity at optical frequencies that can be modeled by the empirical formula $\varepsilon = 5.7 - 9^2/\omega^2 + \mathrm{i}0.4$ (ω in eV units) and has negative dielectric permittivity, while silica has a positive dielectric permittivity. It can

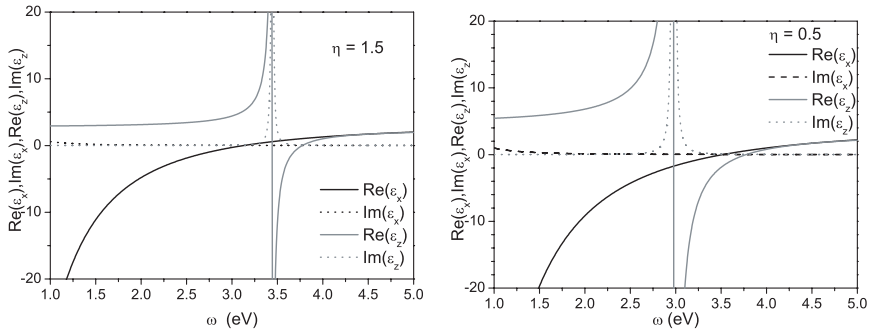

(a) $\eta = 1.5$. (b) $\eta = 0.5$.

Figure 2.5 Anisotropic effective dielectric permittivities of a layered system consisting of alternating layers of silver and silica for two different values of η. The electric permittivity of silver is given by the empirical formula $\varepsilon = 5.7 - 9^2/\omega^2 + \mathrm{i}0.4$, which fits the experimental data reasonably well. The dielectric properties of silica are modeled via the Sellmeier's three resonance formula (Buck 2004).

be clearly seen for the layered stack with $\eta = 1.5$ (more silica layer thickness) that ε_x and ε_z can have opposite signs in certain frequency bands. The effective medium permittivities of one such layered composite, where the dielectric permittivities and the thicknesses ratio of the layers are given in the figure caption, are shown in Fig. 2.5(a). At low frequencies ($\omega < 3.2eV$), $\varepsilon_x < 0$ and $\varepsilon_z > 0$. In the frequency bandwidth $3.5\text{eV} < \omega < 3.73$, $\varepsilon_x > 0$ while $\varepsilon_z < 0$. This anisotropy can be fruitfully used to obtain subwavelength image resolution as discussed in Chapter 8. Fine control over the behavior of the effective medium parameters is possible by changing the relative layer thicknesses. As shown in Fig. 2.5(b), for $\eta = 0.5$ (more silver layer thickness), both ε_x and ε_z have negative permittivity in the high frequency band. It should be stressed that even though the final expressions for ε involve only the ratio η and not the individual layer thicknesses, the expressions are valid only in the limit of extremely small layer thickness. For layers of finite thickness, the modulation of the fields inside the layers needs to be accounted for.

2.5.3 Averaging the internal fields in periodic media

Generally, in a given metamaterial, the structures are much more complex than spheres or ellipsoids. Furthermore, many metamaterials consist of units arranged on a periodic lattice. While the polarizabilities of the individual metamaterial units can be calculated or measured via the scattered fields, the average fields obtained via Maxwell-Garnett type theories do not often satisfy the conditions of continuity on the fields across the system in a rigorous man-

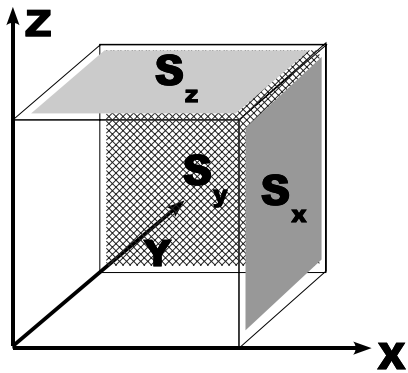

Figure 2.6 The procedure for averaging the internal microscopic fields consists of averaging the **E** and **H** fields over the edges of the unit cell of the simple cubic lattice, while the **D** and **B** fields are averaged over a face S_x for the x-component, and similarly for the other components.

ner. Consider subsequently a way of computing averages for electromagnetic fields in a lattice as discussed in Pendry et al. (1999). Let us start with the Maxwell equations in material media

$$\nabla \times \mathbf{E} = -\frac{\partial \mathbf{B}}{\partial t},$$
$$\nabla \times \mathbf{H} = \frac{\partial \mathbf{D}}{\partial t}.$$

These can be recast in integral form

$$\oint_C \mathbf{E} \cdot \mathrm{d}\mathbf{l} = -\frac{\partial}{\partial t} \int_S \mathbf{B} \cdot \mathrm{d}\sigma, \tag{2.71}$$
$$\oint_C \mathbf{H} \cdot \mathrm{d}\mathbf{l} = \frac{\partial}{\partial t} \int_S \mathbf{D} \cdot \mathrm{d}\sigma, \tag{2.72}$$

where S is the open surface bound by the closed curve C.

These equations themselves suggest a way of averaging the electromagnetic fields. Consider for simplicity that we have a simple cubic lattice for the metamaterial as shown in Fig. 2.6. The averaged fields $\mathbf{E}_{\text{eff}}$ and $\mathbf{H}_{\text{eff}}$ are

defined by averaging the **E** and **H** along the sides of the unit cell:

$$E_{\text{eff}}^{(x)} = \frac{1}{a}\int_{(0,0,0)}^{(a,0,0)} E_x \mathrm{d}x, \quad E_{\text{eff}}^{(y)} = \frac{1}{a}\int_{(0,0,0)}^{(0,a,0)} E_y \mathrm{d}y, \quad E_{\text{eff}}^{(z)} = \frac{1}{a}\int_{(0,0,0)}^{(0,0,a)} E_z \mathrm{d}z, \tag{2.73}$$

$$H_{\text{eff}}^{(x)} = \frac{1}{a}\int_{(0,0,0)}^{(a,0,0)} H_x \mathrm{d}x, \quad H_{\text{eff}}^{(y)} = \frac{1}{a}\int_{(0,0,0)}^{(0,a,0)} H_y \mathrm{d}y, \quad H_{\text{eff}}^{(z)} = \frac{1}{a}\int_{(0,0,0)}^{(0,0,a)} H_z \mathrm{d}z. \tag{2.74}$$

Similarly, the $\mathbf{D}_{\text{eff}}$ and $\mathbf{B}_{\text{eff}}$ are defined by averaging them over the faces of the unit cell:

$$D_{\text{eff}}^{(x)} = \frac{1}{a^2}\int_{S_x} D_x \mathrm{d}\sigma_x, \qquad D_{\text{eff}}^{(y)} = \frac{1}{a^2}\int_{S_y} D_y \mathrm{d}\sigma_y, \qquad D_{\text{eff}}^{(z)} = \frac{1}{a^2}\int_{S_z} D_z \mathrm{d}\sigma_z, \tag{2.75}$$

$$B_{\text{eff}}^{(x)} = \frac{1}{a^2}\int_{S_x} B_x \mathrm{d}\sigma_x, \qquad B_{\text{eff}}^{(y)} = \frac{1}{a^2}\int_{S_y} B_y \mathrm{d}\sigma_y, \qquad B_{\text{eff}}^{(z)} = \frac{1}{a^2}\int_{S_z} B_z \mathrm{d}\sigma_z. \tag{2.76}$$

where S_x is the face in the yz plane, S_y is the face in the zx plane and S_z is the face in the xy plane. The averaged fields then relate the ε and μ component-wise. There is only one restriction in this procedure: that the unit cell boundaries should not intersect any of the structures contained within so that the continuity of the parallel components of $\mathbf{E}_{\text{eff}}$ and $\mathbf{H}_{\text{eff}}$ across the cell boundaries is maintained. In the case of periodically structured materials, the periodicity implies that the averaging need not be carried over orientational and density fluctuations in the metamaterial.

Consider the system of wires and rings shown in Fig. 2.1. It would be typical to average the H field along a line normal to the rings and along the edge of the cubic cell where the near-fields due to the rings are not very large. But the average for the B field would be across the area of the ring and would pick up the large fields due to the rings. Thus, to create a large effect on the effective medium parameters, we should design structures with large inhomogeneous fields. For sizes of the unit cell comparable to the wavelength, homogenization breaks down. This is automatically reflected in this procedure whereby the averages of different unit cells located at different points in the metamaterial yield different results. This procedure can also be easily extended to the retrieval of bianisotropic parameters (Smith and Pendry 2006).

2.6 Generalization to anisotropic and bianisotropic media

The information provided by the forward model as a set of reflection and transmission coefficients (for various incidences, polarizations, and frequencies if necessary) needs to be processed in an inversion algorithm. Typically, one needs to minimize the complex difference

$$\min\left(R_{\text{mea}} - R_{\text{simu}}(\bar{\bar{\varepsilon}}, \bar{\bar{\mu}})\right), \tag{2.77}$$

where R_{mea} is the measured reflection coefficient (or obtained from the forward model) and R_{simu} is the calculated reflection coefficient for a given model as function of variable parameters. A similar minimization is performed on the transmission coefficient, and the constitutive dyads that achieve the minimum in a certain sense are chosen as the retrieved values.

The process of minimization therefore requires the possibility of computing R_{simu} and T_{simu} for the constitutive dyads chosen as the model of the metamaterial. The minimization can then be performed in essentially two ways:

1. Numerically, the minimization is transformed into an optimization problem that can be addressed with various methods such as genetic algorithms, differential evolution, and other deterministic or non-deterministic methods (the efficacy of the method depending on the complexity of the problem, the more complex the problem and the larger the number local minima to avoid).

2. Analytically, if R_{simu} and T_{simu} are known in closed-form (which is possible in some cases), inversion formulae can be obtained in order to solve for the constitutive parameters. The complexity of the formulae as well as of the mathematical derivations increases with the complexity of the model.

The necessity of computing R_{simu} and T_{simu} for many inputs (as the search algorithm progresses) essentially rules out the possibility of using a direct numerical approach. The latter are usually very flexible and powerful in terms of their simulation capabilities, but this flexibility also often comes at the expense of computational time: when hundreds or thousands of iterations are needed, this may become an important disadvantage. Whenever possible, it is therefore more desirable to develop a method that is less general but which addresses the specific problem under consideration in an efficient manner. In the next section, we present such a method for the computation of the fields in layered media where the constitutive parameters can be arbitrary bian-

isotropic tensors, as a generalization of the anisotropic case treated in Chew (1990).‡

2.6.1 Forward model

The following method is a generalization of the common Transfer Matrix Method for layered media (Born and Wolf 1999) for the general case when the materials can be anisotropic and bianisotropic. Let us consider a homogeneous layered medium in the $\hat{z}$ direction, where each layer is characterized by potentially fully populated bianisotropic tensors, as shown in Fig. 2.7.

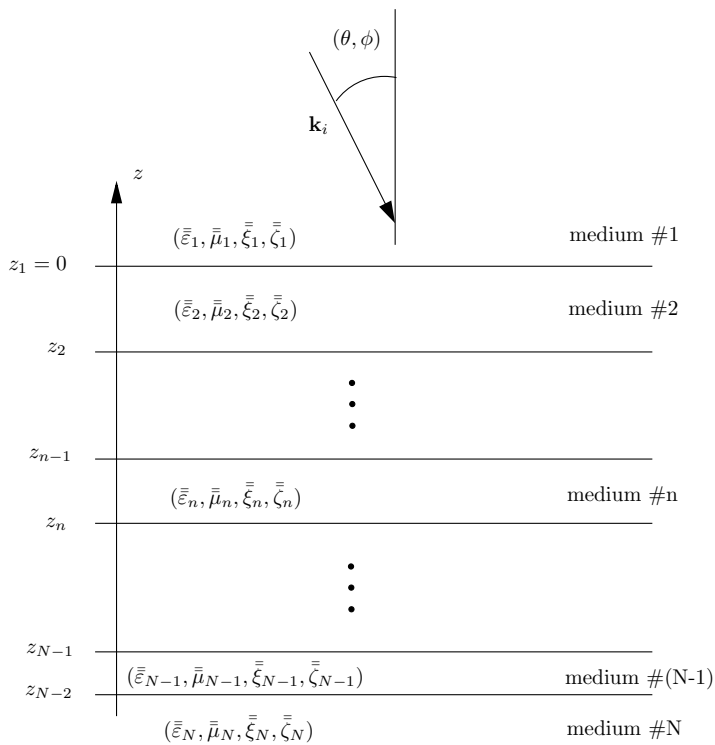

Figure 2.7 Configuration of the problem: a plane wave with wave vector $\mathbf{k}_i$ is incident with the polar angles (θ, ϕ) onto a multi-layered medium of arbitrary constitutive bianisotropic tensors.

‡It should be noted that to our knowledge, a numerical package does not exist that is able to compute the field in layered media when the bianisotropic parameters are all random tensors. However, some results in this direction have been presented in Ouchetto et al. (2006).

Assuming an $e^{-\mathrm{i}\omega t}$ dependency, the source free Maxwell equations are written as

$$\nabla \times \mathbf{E}(\mathbf{r}) = \ \mathrm{i}\omega \mathbf{B}(\mathbf{r})\,, \tag{2.78a}$$

$$\nabla \times \mathbf{H}(\mathbf{r}) = -\,\mathrm{i}\omega \mathbf{D}(\mathbf{r})\,, \tag{2.78b}$$

with the constitutive relations in the Telegen representation (Weiglhofer 2003)

$$\mathbf{D}(\mathbf{r}) = \bar{\bar{\varepsilon}} \cdot \mathbf{E}(\mathbf{r}) + \bar{\bar{\xi}} \cdot \mathbf{H}(\mathbf{r})\,, \tag{2.79a}$$

$$\mathbf{B}(\mathbf{r}) = \bar{\bar{\mu}} \cdot \mathbf{H}(\mathbf{r}) + \bar{\bar{\zeta}} \cdot \mathbf{E}(\mathbf{r})\,. \tag{2.79b}$$

The constitutive parameters $\bar{\bar{\varepsilon}}$, $\bar{\bar{\mu}}$, $\bar{\bar{\xi}}$, and $\bar{\bar{\zeta}}$ are arbitrary random tensors, potentially fully populated, and homogeneous within each layer. In addition, within this section, it is understood that they are absolute values, related to the relative quantities, denoted by the subscript 'r', by

$$\bar{\bar{\varepsilon}} = \varepsilon_0 \bar{\bar{\varepsilon}}_r\,, \qquad \bar{\bar{\mu}} = \mu_0 \bar{\bar{\mu}}_r\,, \qquad \bar{\bar{\xi}} = \bar{\bar{\xi}}_r / c\,, \qquad \bar{\bar{\zeta}} = \bar{\bar{\zeta}}_r / c\,. \tag{2.80}$$

The dispersion relation within these general media can be obtained by eliminating all the vectors but $\mathbf{E}$ and setting the dispersion relation of the matrix operating on $\mathbf{E}$ equal to zero. One simply obtains

$$\left| \omega^2 \bar{\bar{\varepsilon}} + \left(\bar{\bar{k}} + \omega \bar{\bar{\xi}} \right) \cdot \bar{\bar{\mu}}^{-1} \cdot \left(\bar{\bar{k}} - \omega \bar{\bar{\zeta}} \right) \right| = 0\,, \tag{2.81}$$

where $\bar{\bar{k}} = \mathbf{k} \times \bar{\bar{I}}_3$. Using the preferential $\hat{z}$ direction to split the tensors into transverse and longitudinal parts, we write

$$\bar{\bar{\varepsilon}} = \begin{bmatrix} \bar{\bar{\varepsilon}}_{ss} & \bar{\bar{\varepsilon}}_{sz} \\ \bar{\bar{\varepsilon}}_{zs} & \varepsilon_{zz} \end{bmatrix} \tag{2.82}$$

and similarly for $\bar{\bar{\mu}}$, $\bar{\bar{\xi}}$, $\bar{\bar{\zeta}}$, which, upon inserting into the constitutive relations (2.79) and the Maxwell equations (2.78), yield

$$\begin{aligned} \nabla_s \times \hat{z} E_z(\mathbf{r}) + \hat{z} \times \frac{\partial}{\partial_z} \mathbf{E}_s(\mathbf{r}) = \ & \mathrm{i}\omega \bar{\bar{\mu}}_{ss} \cdot \mathbf{H}_s(\mathbf{r}) + \mathrm{i}\omega \bar{\bar{\mu}}_{sz} \cdot \hat{z} H_z(\mathbf{r}) \\ & + \mathrm{i}\omega \bar{\bar{\zeta}}_{ss} \cdot \mathbf{E}_s(\mathbf{r}) + \mathrm{i}\omega \bar{\bar{\zeta}}_{sz} \cdot \hat{z} E_z(\mathbf{r})\,, \end{aligned} \tag{2.83a}$$

$$\nabla_s \times \mathbf{E}_s(\mathbf{r}) = \ \mathrm{i}\omega \bar{\bar{\mu}}_{zs} \cdot \mathbf{H}_s(\mathbf{r}) + \mathrm{i}\omega \mu_{zz} \hat{z} H_z(\mathbf{r}) + \mathrm{i}\omega \bar{\bar{\zeta}}_{zs} \cdot \mathbf{E}_s(\mathbf{r}) + \mathrm{i}\omega \zeta_{zz} \hat{z} E_z(\mathbf{r})\,, \tag{2.83b}$$

$$\begin{aligned} \nabla_s \times \hat{z} H_z(\mathbf{r}) + \hat{z} \times \frac{\partial}{\partial_z} \mathbf{H}_s(\mathbf{r}) = \ & -\mathrm{i}\omega \bar{\bar{\varepsilon}}_{ss} \cdot \mathbf{E}_s(\mathbf{r}) - \mathrm{i}\omega \bar{\bar{\varepsilon}}_{sz} \cdot \hat{z} E_z(\mathbf{r}) \\ & - \mathrm{i}\omega \bar{\bar{\xi}}_{ss} \cdot \mathbf{H}_s(\mathbf{r}) - \mathrm{i}\omega \bar{\bar{\xi}}_{sz} \cdot \hat{z} H_z(\mathbf{r})\,, \end{aligned} \tag{2.83c}$$

$$\nabla_s \times \mathbf{H}_s(\mathbf{r}) = \ -\mathrm{i}\omega \bar{\bar{\varepsilon}}_{zs} \cdot \mathbf{E}_s(\mathbf{r}) - \mathrm{i}\omega \varepsilon_{zz} \hat{z} E_z(\mathbf{r}) - \mathrm{i}\omega \bar{\bar{\xi}}_{zs} \cdot \mathbf{H}_s(\mathbf{r}) - \mathrm{i}\omega \xi_{zz} \hat{z} H_z(\mathbf{r})\,. \tag{2.83d}$$

The solutions in each homogeneous layer are plane waves of the form $e^{\mathrm{i}\mathbf{k}_s\cdot\mathbf{r}_s}$ so that ∇_s is replaced by $\mathrm{i}\mathbf{k}_s$ in Eqs. (2.83). Taking $\hat{z}$ as the propagation direction, the transverse components can then be separated from the longitudinal ones as

$$\mathbf{E}_z(\mathbf{r}) = \frac{1}{D}\left[-\frac{\xi_{zz}}{\omega}\mathbf{k}_s\times\bar{\bar{I}}_3\cdot\ +\xi_{zz}\bar{\bar{\zeta}}_{zs}\cdot\ -\mu_{zz}\bar{\bar{\varepsilon}}_{zs}\cdot\right]\mathbf{E}_s(\mathbf{r}) + \frac{1}{D}\left[\xi_{zz}\bar{\bar{\mu}}_{zs}\cdot\ -\frac{\mu_{zz}}{\omega}\mathbf{k}_s\times\bar{\bar{I}}_3\cdot\ -\mu_{zz}\bar{\bar{\xi}}_{zs}\cdot\right]\mathbf{H}_s(\mathbf{r})\,, \tag{2.84a}$$

$$\mathbf{H}_z(\mathbf{r}) = \frac{1}{D}\left[\frac{\varepsilon_{zz}}{\omega}\mathbf{k}_s\times\bar{\bar{I}}_3\cdot\ -\varepsilon_{zz}\bar{\bar{\zeta}}_{zs}\cdot\ +\zeta_{zz}\bar{\bar{\varepsilon}}_{zs}\cdot\right]\mathbf{E}_s(\mathbf{r}) + \frac{1}{D}\left[-\varepsilon_{zz}\bar{\bar{\mu}}_{zs}\cdot\ +\frac{\zeta_{zz}}{\omega}\mathbf{k}_s\times\bar{\bar{I}}_3\cdot\ +\zeta_{zz}\bar{\bar{\xi}}_{zs}\cdot\right]\mathbf{H}_s(\mathbf{r})\,, \tag{2.84b}$$

where

$$\mathbf{k}_s\times\bar{\bar{I}}_3 = \begin{pmatrix} 0 & 0 & k_y\\ 0 & 0 & -k_x\\ -k_y & k_x & 0\end{pmatrix} \tag{2.85}$$

$$\text{and } D = (\varepsilon_{zz}\mu_{zz} - \xi_{zz}\zeta_{zz})\,. \tag{2.86}$$

Using Eqs. (2.84) into Eqs. (2.83), the longitudinal components H_z and E_z can be factored out, leaving only an expression in terms of the transverse components and their derivatives:

$$\begin{aligned}\frac{\partial}{\partial_z}\mathbf{E}_s(\mathbf{r}) = \frac{1}{D}\Bigg[&-\frac{\mathrm{i}\xi_{zz}}{\omega}\ \hat{z}\times\bar{\bar{I}}_3\cdot\mathbf{k}_s\times\bar{\bar{I}}_3\cdot\mathbf{k}_s\times\bar{\bar{I}}_3\cdot\ +\mathrm{i}\xi_{zz}\ \hat{z}\times\bar{\bar{I}}_3\cdot\mathbf{k}_s\times\bar{\bar{I}}_3\cdot\bar{\bar{\zeta}}_{zs}\cdot\\ &-\mathrm{i}\mu_{zz}\ \hat{z}\times\bar{\bar{I}}_3\cdot\mathbf{k}_s\times\bar{\bar{I}}_3\cdot\bar{\bar{\varepsilon}}_{zs}\cdot\ -\mathrm{i}\omega D\hat{z}\times\bar{\bar{I}}_3\cdot\bar{\bar{\zeta}}_{ss}\cdot\\ &-\mathrm{i}\varepsilon_{zz}\ \hat{z}\times\bar{\bar{I}}_3\cdot\bar{\bar{\mu}}_{sz}\cdot\mathbf{k}_s\times\bar{\bar{I}}_3\cdot\ +\mathrm{i}\omega\varepsilon_{zz}\ \hat{z}\times\bar{\bar{I}}_3\cdot\bar{\bar{\mu}}_{sz}\cdot\bar{\bar{\zeta}}_{zs}\cdot\\ &-\mathrm{i}\omega\zeta_{zz}\ \hat{z}\times\bar{\bar{I}}_3\cdot\bar{\bar{\mu}}_{sz}\cdot\bar{\bar{\varepsilon}}_{zs}\cdot\ +\mathrm{i}\xi_{zz}\ \hat{z}\times\bar{\bar{I}}_3\cdot\bar{\bar{\zeta}}_{sz}\cdot\mathbf{k}_s\times\bar{\bar{I}}_3\cdot\\ &-\mathrm{i}\omega\xi_{zz}\ \hat{z}\times\bar{\bar{I}}_3\cdot\bar{\bar{\zeta}}_{sz}\cdot\bar{\bar{\zeta}}_{zs}\cdot\ +\mathrm{i}\omega\mu_{zz}\ \hat{z}\times\bar{\bar{I}}_3\cdot\bar{\bar{\zeta}}_{sz}\cdot\bar{\bar{\varepsilon}}_{zs}\cdot\Bigg]\mathbf{E}_s(\mathbf{r})\\ +\frac{1}{D}\Bigg[&\mathrm{i}\xi_{zz}\ \hat{z}\times\bar{\bar{I}}_3\cdot\mathbf{k}_s\times\bar{\bar{I}}_3\cdot\bar{\bar{\mu}}_{zs}\cdot\ -\frac{\mathrm{i}\mu_{zz}}{\omega}\ \hat{z}\times\bar{\bar{I}}_3\cdot\mathbf{k}_s\times\bar{\bar{I}}_3\cdot\mathbf{k}_s\times\bar{\bar{I}}_3\cdot\\ &-\mathrm{i}\mu_{zz}\ \hat{z}\times\bar{\bar{I}}_3\cdot\mathbf{k}_s\times\bar{\bar{I}}_3\cdot\bar{\bar{\xi}}_{zs}\cdot\ -\mathrm{i}\omega D\hat{z}\times\bar{\bar{I}}_3\cdot\bar{\bar{\mu}}_{ss}\cdot\\ &+\mathrm{i}\omega\varepsilon_{zz}\ \hat{z}\times\bar{\bar{I}}_3\cdot\bar{\bar{\mu}}_{sz}\cdot\bar{\bar{\mu}}_{zs}\cdot\ -\mathrm{i}\zeta_{zz}\ \hat{z}\times\bar{\bar{I}}_3\cdot\bar{\bar{\mu}}_{sz}\cdot\mathbf{k}_s\times\bar{\bar{I}}_3\cdot\\ &-\mathrm{i}\omega\zeta_{zz}\ \hat{z}\times\bar{\bar{I}}_3\cdot\bar{\bar{\mu}}_{sz}\cdot\bar{\bar{\xi}}_{zs}\cdot\ -\mathrm{i}\omega\xi_{zz}\ \hat{z}\times\bar{\bar{I}}_3\cdot\bar{\bar{\zeta}}_{sz}\cdot\bar{\bar{\mu}}_{zs}\cdot\\ &+\mathrm{i}\mu_{zz}\ \hat{z}\times\bar{\bar{I}}_3\cdot\bar{\bar{\zeta}}_{sz}\cdot\mathbf{k}_s\times\bar{\bar{I}}_3\cdot\ +\mathrm{i}\omega\mu_{zz}\ \hat{z}\times\bar{\bar{I}}_3\cdot\bar{\bar{\zeta}}_{sz}\cdot\bar{\bar{\xi}}_{zs}\cdot\Bigg]\mathbf{H}_s(\mathbf{r})\,,\end{aligned} \tag{2.87}$$

where

$$\hat{z} \times \bar{\bar{I}}_3 = \begin{pmatrix} 0 & -1 & 0 \\ 1 & 0 & 0 \\ 0 & 0 & 0 \end{pmatrix} . \tag{2.88}$$

Note that the second equation expressing $\partial \mathbf{H}_s(\mathbf{r})/\partial z$ is directly obtained from Eqs. (2.87) and from the duality condition so that we do not write it explicitly here. The two equations thus obtained can then be gathered in a matrix form as (Berreman 1972, Chew 1990, Norgen 1997):

$$\frac{\partial}{\partial z} \begin{pmatrix} \mathbf{E}_s(\mathbf{r}) \\ \mathbf{H}_s(\mathbf{r}) \end{pmatrix} \begin{pmatrix} \bar{\bar{F}}_{11} & \bar{\bar{F}}_{12} \\ \bar{\bar{F}}_{21} & \bar{\bar{F}}_{22} \end{pmatrix} \cdot \begin{pmatrix} \mathbf{E}_s(\mathbf{r}) \\ \mathbf{H}_s(\mathbf{r}) \end{pmatrix} , \tag{2.89}$$

where each $\bar{\bar{F}}_{ij}$ ($\{i,j\} \in \{1,2\}$) is the top-left 2×2 matrix obtained from Eqs. (2.87) and its dual (a 2×2 system that is obtained by discarding the zero components in Eqs. (2.87)). Written in vectorial form, the system (2.89) is a simple ordinary differential equation that admits exponential functions as solutions. Being a 4×4 system, it admits four eigenvalues, four eigenvectors, and four coefficients that need to be determined by applying the boundary conditions at the interfaces between all the layers. The eigenvectors correspond to the polarization states of the transverse electromagnetic field components, while the eigenvalues correspond to the wave-vectors supported by the medium. For example, if we consider an isotropic homogeneous medium, the four solutions correspond to the TE and TM polarizations (which happen to share similar wave-vectors) propagating in the upward and downward directions.

The eigenvectors and eigenvalues can thus be sorted so that the first two correspond to upward propagating waves while the last two correspond to downward propagating waves. For reasons that will be made clear in Chapter 5 in order to avoid all confusion in media with negative constitutive parameters, this ordering should be performed by examining the direction of power propagation (the Poynting vector) rather than just the sign of the wavenumbers.

Upon defining the vector $\mathbf{V}(z)$ as the 4×1 vector $[\mathbf{E}_s(\mathbf{r}); \mathbf{H}_s(\mathbf{r})]^T$ (where the subscript T denotes the transpose operator), we can rewrite Eq. (2.89) as $\frac{\partial}{\partial z}\mathbf{V}(z) = \bar{\bar{F}} \cdot \mathbf{V}(z)$, where the 4×4 tensor $\bar{\bar{F}}$ is straightforwardly defined from Eq. (2.89). Following the notation of Chew (1990), we denote by $\bar{\bar{a}}_n$ the tensor containing the four (sorted) eigenvectors of medium $\#n$, and $\bar{\bar{\beta}}_n$ the diagonal 4×4 tensor containing the four (sorted) eigenvalues of medium $\#n$. Thus, the transverse polarization states in medium n ($\mathbf{V}_n(z)$) are written as

$$\text{medium 1:} \quad \mathbf{V}_1(z) = \bar{\bar{a}}_1 \cdot e^{\mathrm{i}\bar{\bar{\beta}}_1 z} \cdot \begin{bmatrix} \bar{\bar{R}} \\ \bar{\bar{I}}_2 \end{bmatrix} \cdot \begin{bmatrix} A_{31} \\ A_{41} \end{bmatrix} , \tag{2.90a}$$

$$\text{medium } n\text{:} \quad \mathbf{V}_n(z) = \bar{\bar{a}}_n \cdot e^{\mathrm{i}\bar{\bar{\beta}}_n z} \cdot \mathbf{A}_n , \tag{2.90b}$$

$$\mathbf{V}_n(z) = \bar{\bar{P}}_n(z, z_{n-1}) \cdot \mathbf{V}_n(z_{n-1}) . \tag{2.90c}$$

A_{31} and A_{41} are the amplitudes of the two polarizations of the down-going incident waves and are therefore known (if the first medium is free-space, A_{31} and A_{41} represent the amplitudes of the TE and TM incident waves). $\mathbf{A}_n$ is a 4×1 vector containing the coefficients of the four waves in medium n, and $\bar{\bar{P}}$ represents the propagator (or transfer) matrix (Chew 1990) defined as

$$\bar{\bar{P}}_n(z, z_{n-1}) = \bar{\bar{a}}_n \cdot e^{\mathrm{i}\bar{\bar{\beta}}_n(z-z_{n-1})} \cdot \bar{\bar{a}}_n^{-1} . \tag{2.91}$$

These expressions can be directly used in the boundary conditions $\mathbf{V}_n(z_{n-1}) = \mathbf{V}_{n-1}(z_{n-1})$ expressing the continuity of the tangential electric and magnetic components and providing a recurrence relation in the vector $\mathbf{V}$:

$$\begin{aligned}
&\mathbf{V}_1(z_1) = \mathbf{V}_2(z_1) = \ \bar{\bar{P}}_2(z_1, z_2) \cdot \mathbf{V}_2(z_2) \,, \\
&\mathbf{V}_2(z_2) = \mathbf{V}_3(z_2) = \ \bar{\bar{P}}_3(z_2, z_3) \cdot \mathbf{V}_3(z_3) \,, \\
&\quad \vdots \\
&\mathbf{V}_{n-2}(z_{n-2}) = \mathbf{V}_{n-1}(z_{n-2}) = \ \bar{\bar{P}}_{n-1}(z_{n-2}, z_{n-1}) \cdot \mathbf{V}_{n-1}(z_{n-1}) \,, \\
&\mathbf{V}_{n-1}(z_{n-1}) = \mathbf{V}_n(z_{n-1}) \,.
\end{aligned} \tag{2.92}$$

Combining all the terms, we get

$$\begin{aligned}
\mathbf{V}_1(z_1) &= \bar{\bar{P}}_2(z_1, z_2) \cdot \bar{\bar{P}}_3(z_2, z_3) \cdot \ldots \cdot \bar{\bar{P}}_{n-1}(z_{n-2}, z_{n-1}) \cdot \mathbf{V}_n(z_{n-1}) \\
&= \bar{\bar{P}}_A(z_1, \ldots, z_{n-1}) \cdot \mathbf{V}_n(z_{n-1}) \,.
\end{aligned} \tag{2.93}$$

Upon using Eqs. (2.90a) and (2.90c), the state vector for the transverse components is written as

$$\mathbf{V}_n(z) = \ \bar{\bar{P}}_n(z, z_{n-1}) \cdot \bar{\bar{P}}_A^{-1}(z_1, \ldots, z_{n-1}) \cdot \bar{\bar{a}}_1 \cdot e^{\mathrm{i}\bar{\bar{\beta}}_1 z_1} \cdot \begin{bmatrix} \bar{\bar{R}} \\ \bar{\bar{I}}_2 \end{bmatrix} \cdot \begin{bmatrix} A_{31} \\ A_{41} \end{bmatrix} . \tag{2.94}$$

The last medium is treated equally and yields

$$\mathbf{V}_N(z) = \bar{\bar{a}}_N \cdot e^{\mathrm{i}\bar{\bar{\beta}}_N z} \cdot \begin{bmatrix} 0 \\ \bar{\bar{T}} \end{bmatrix} \cdot \begin{bmatrix} A_{31} \\ A_{41} \end{bmatrix} . \tag{2.95}$$

In these equations, $\bar{\bar{R}}$ and $\bar{\bar{T}}$ are 2×2 dyads that need to be solved for. Still assuming free-space as the surrounding medium, the polarization in the first and last medium can be decomposed into TE and TM so that the various components of the reflection and transmission dyads correspond to TE/TM reflection (transmission) due to a TE/TM incidence. Writing the recurrence formula from the first to the last medium,

$$\bar{\bar{a}}_1 \cdot e^{\mathrm{i}\bar{\bar{\beta}}_1 z_1} \cdot \begin{bmatrix} \bar{\bar{R}} \\ \bar{\bar{I}}_2 \end{bmatrix} \bar{\bar{P}}_A(z_1, \ldots, z_{N-1}) \cdot \bar{\bar{a}}_N \cdot e^{\mathrm{i}\bar{\bar{\beta}}_N z_{N-1}} \begin{bmatrix} 0 \\ \bar{\bar{T}} \end{bmatrix} \tag{2.96}$$

produces a matrix equation that can be solved for $\bar{\bar{R}}$ and $\bar{\bar{T}}$. Using Eqs. (2.90a) and (2.84), the fields in each medium can be entirely determined.

The method presented in this section is therefore able to produce not only the reflection and transmission dyads but also the field profile in each layer (which is not directly necessary in the retrieval process). The concatenation of 2×2 or 4×4 matrix multiplication makes this method very fast, and thus well suited in an inversion algorithm that requires multiple forward solutions for various inputs.

In addition, the method can be carried out analytically in some simple cases of constitutive tensors in order to obtain closed-form expressions for the reflection and transmission coefficients, necessary for any retrieval algorithm based on analytical solutions. For example, the following expressions can be directly obtained:

1. A half-space interfacing free-space and a biaxial medium, defined by the dyads

$$\bar{\bar{\varepsilon}}_1 = \varepsilon_0 \bar{\bar{I}}_3, \qquad \bar{\bar{\mu}}_1 = \mu_0 \bar{\bar{I}}_3 \tag{2.97a}$$

$$\bar{\bar{\varepsilon}}_2 = \begin{bmatrix} \varepsilon_{2x} & 0 & 0 \\ 0 & \varepsilon_{2y} & 0 \\ 0 & 0 & \varepsilon_{2z} \end{bmatrix}, \qquad \bar{\bar{\mu}}_2 = \begin{bmatrix} \mu_{2x} & 0 & 0 \\ 0 & \mu_{2y} & 0 \\ 0 & 0 & \mu_{2z} \end{bmatrix}. \tag{2.97b}$$

   For $k_y = 0$, the TE coefficients (identified by the 'hs' subscript to denote the half-space case) are expressed as

$$R_{\mathrm{hs}} = \frac{k_{z1}\sqrt{\mu_{2x}\mu_{2z}} - k_{z2}\mu_1}{k_{z1}\sqrt{\mu_{2x}\mu_{2z}} + k_{z2}\mu_1}, \tag{2.98a}$$

$$T_{\mathrm{hs}} = \frac{2k_{z1}\sqrt{\mu_{2x}\mu_{2z}}}{k_{z1}\sqrt{\mu_{2x}\mu_{2z}} + k_{z2}\mu_1}, \tag{2.98b}$$

   where

$$k_{z2}^2 = \omega^2 \varepsilon_{2y}\mu_{2z} - k_x^2 . \tag{2.99}$$

2. A slab of biaxial medium defined by similar constitutive parameters and surrounded by free-space produces a reflection and transmission coefficients that are expressed as

$$R_{\mathrm{slab}} = \frac{R_{\mathrm{hs}}(e^{2\Phi} - 1)}{R_{\mathrm{hs}}^2 e^{2\Phi} - 1}, \qquad T_{\mathrm{slab}} = \frac{R_{\mathrm{hs}}^2 - 1}{R_{\mathrm{hs}}^2 e^{2\Phi} - 1}, \tag{2.100}$$

   where $\Phi = \mathrm{i}k_{z1}d$, d being the thickness of the slab.

3. A slab of bianisotropic medium defined by the following constitutive parameters:

$$\bar{\bar{\varepsilon}}_r = \begin{bmatrix} \varepsilon_{r_{xx}} & 0 & 0 \\ 0 & 1 & 0 \\ 0 & 0 & \varepsilon_{r_{zz}} \end{bmatrix}, \qquad \bar{\bar{\mu}}_r = \begin{bmatrix} 1 & 0 & 0 \\ 0 & \mu_{r_{yy}} & 0 \\ 0 & 0 & 1 \end{bmatrix}, \tag{2.101a}$$

$$\bar{\bar{\xi}}_r = \begin{bmatrix} 0 & 0 & 0 \\ 0 & 0 & 0 \\ 0 & -\mathrm{i}\xi & 0 \end{bmatrix}, \qquad \bar{\bar{\zeta}}_r = \begin{bmatrix} 0 & 0 & 0 \\ 0 & 0 & \mathrm{i}\xi \\ 0 & 0 & 0 \end{bmatrix}. \tag{2.101b}$$

These constitutive dyads correspond to the well-accepted model for the original split ring resonator (Pendry et al. 1999, Smith et al. 2000) (see Fig. 3.8) and have been studied in detail in Marques et al. (2002). The diagonal permittivity and permeability reflect the usual anisotropic property of the metamaterial due to the orientation of the metallic rods and rings. The bianisotropic terms instead are directly related to the shape of the metallic ring. In this case, the presence of oppositely oriented gaps in the two rings induces asymmetric currents and charge distributions in them due to the impinging magnetic field, generating symmetric dipole moments in one direction and asymmetric dipole moments in the orthogonal direction on either side of the ring. The asymmetric components do not cancel out and result in the generation of an electric polarization from an incident magnetic field, directly following the definition of bianisotropy in Eqs. (2.79). Conversely, an electric field propagating in the plane of the ring may impinge on either its symmetric side or its asymmetric side. If impinging on the asymmetric side, the induced current distribution is asymmetric, creating a current flow and therefore a magnetic field. We therefore have the creation of a magnetic field due to the interaction of the structure with the impinging electric field. Note, however, that the original ring is composed of two interlaced split-rings, whereas the explanation of the bianisotropic effect only requires one split-ring. The presence of the second split-ring would require a rigorous consideration of coupling and fringing fields between the two rings for a more accurate quantitative description. A methodology for including these effects is presented in Section 3.2.7.

Given the orientation of the rings in the metamaterial, it is more natural to look for a TM polarization (H fields normal to the plane of the rings) in this case. The reflection coefficients for both the half-space and slab

cases are given by

$$R_{\mathrm{hs}} = \frac{k_{z1}\varepsilon_{2z} - k_{z2}\varepsilon_1}{k_{z1}\varepsilon_{2z} + k_{z2}\varepsilon_1}\,, \tag{2.102a}$$

$$R_{\mathrm{slab}} = \frac{R_{\mathrm{hs}}\left(e^{2\Phi} - 1\right)}{\left(R_{\mathrm{hs}}\right)^2 e^{2\Phi} - 1}\,, \tag{2.102b}$$

where

$$k_{z2}^2 = \frac{\varepsilon_{2x}}{\varepsilon_{2z}}\left(\omega^2\varepsilon_{2z}\mu_{2y} - k_x^2 - \omega^2\xi^2\right)\,, \tag{2.103a}$$

$$\Phi = \mathrm{i}k_{z2}d\,. \tag{2.103b}$$

2.6.2 Inversion algorithm

Two approaches can be considered for the inversion of the tensorial parameters: an analytical one where, like in the biaxial case, one looks for a formula yielding directly the unknown parameters, and a numerical one, typically based on an optimization scheme and a search algorithm. The analytical approach has the appeal of providing the exact solution without ambiguity and almost instantaneously. However, the situations where an inversion formula can be obtained is usually limited to simple tensors for which an analytical derivation is still manageable. The numerical approach, on the other hand, can always be applied but does not offer the guarantee of convergence and may find local minima as the solution. This can be somehow avoided by the use of both deterministic and stochastic algorithms, even though the final results still need to be checked for consistency. In addition, the numerical minimization of such highly nonlinear problems often requires very long computation time without providing the assurance of the existence of a unique solution.

In the case of the bianisotropy governed by Eqs. (2.101), the tensors are simple enough to allow for an analytical solution and, more interestingly, this model corresponds to the effective medium of a widely used split-ring resonator, as shown in Marques et al. (2002). The unknowns to be solved for (ε_x, ε_y, ε_z, μ_x, μ_y, μ_z, ξ), require multiple equations that can be obtained by varying the polarization and incidence angles with respect to the unit cell of the metamaterial. The number of unknowns and therefore the number of equations required depend on the initial assumption: for lossless media seven unknowns need to be determined whereas fourteen need to be determined in the case of a lossy medium (note that if ξ is *a priori* known to be real, we still treat it as complex and expect to retrieve a zero imaginary part). The incidences and polarizations that provide the necessary information are illustrated in Fig. 2.8, labeled as TE_i and TM_i ($i = 1, 2, 3$). The bianisotropic

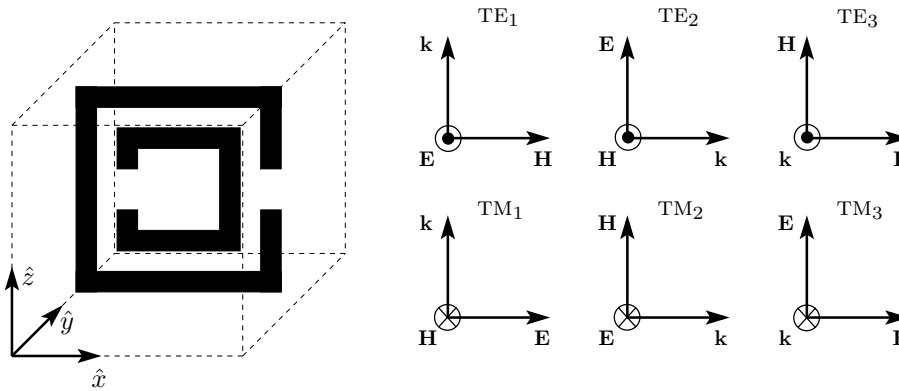

Figure 2.8 Illustration of multiple incidences and polarizations impinging on a unit cell of bianisotropic metamaterial governed by the model of Eqs. (2.101).

Table 2.1 Redefinition of the impedance and the index of refraction for the incidences defined in Fig. 2.8. Note that the TE$_2$ case is lossless.

Case	Dispersion relation	Impedance	Index of refraction
TE$_1$	$k_z^2{=}k_0^2\varepsilon_y\mu_x$	$\sqrt{\mu_x/\varepsilon_y}$	$\sqrt{\varepsilon_y\mu_x}$
TE$_2$	$k_x^2{=}k_0^2(\varepsilon_z\mu_y{-}\xi^2)$	$\mu_y/(\sqrt{\varepsilon_z\mu_y{-}\xi^2}{+}\mathrm{i}\xi)$	$\sqrt{\varepsilon_z\mu_y{-}\xi^2}$
TE$_3$	$k_y^2{=}k_0^2\varepsilon_x\mu_z$	$\sqrt{\mu_z/\varepsilon_x}$	$\sqrt{\varepsilon_x\mu_z}$
TM$_1$	$k_z^2{=}k_0^2(\varepsilon_x\mu_y{-}\varepsilon_x/\varepsilon_z\xi^2)$	$\varepsilon_x/\sqrt{\varepsilon_x\mu_y{-}\varepsilon_x/\varepsilon_z\xi^2}$	$\sqrt{\varepsilon_x\mu_y{-}\varepsilon_x/\varepsilon_z\xi^2}$
TM$_2$	$k_x^2{=}k_0^2\varepsilon_y\mu_z$	$\sqrt{\varepsilon_y/\mu_z}$	$\sqrt{\varepsilon_y\mu_z}$
TM$_3$	$k_y^2{=}k_0^2(\varepsilon_z\mu_x{-}\mu_x/\mu_y\xi^2)$	$\varepsilon_z/\sqrt{\varepsilon_z\mu_x{-}\mu_x/\mu_y\xi^2}$	$\sqrt{\varepsilon_z\mu_x{-}\mu_x/\mu_y\xi^2}$

property of this ring comes from the coupling between the y component of the magnetic field that produces an imbalance of charges via induced currents and hence, an electric field, and conversely, between the z component of the electric field that produces a magnetic field by driving a current via the polarization charges. Consequently, out of the six incidences considered, only three of them see the bianisotropy (TE$_2$, TM$_1$, TM$_3$) and only one (TE$_2$) sees it for both the electric and magnetic field (since it contains both E_z and H_y). The other incidences propagate through the medium as if it were isotropic, and therefore the retrieval of the associated constitutive parameters can be performed directly using the method presented in the previous section, providing that the index of refraction and the impedance are properly redefined (see Tab. 2.1 and also Appendix B).

Incidence TE$_2$ requires a particular attention since it contains both an H_y component that induces an electric dipole in the $\hat{z}$ direction, and an E_z component that induces a magnetic dipole in the $\hat{y}$ direction. Using the method

presented in Section 2.6.1, the S_{11} and S_{21} parameters are found to be

$$S_{11} = \frac{\frac{\mu_{2y}-k_{2x}/k_0-\mathrm{i}\xi}{\mu_{2y}+k_{2x}/k_0+\mathrm{i}\xi}(1-e^{2\mathrm{i}k_{2x}d})}{1-\frac{(k_{2x}/k_0-\mu_{2y})^2+\xi^2}{(k_{2x}/k_0+\mu_{2y})^2+\xi^2}e^{2\mathrm{i}k_{2x}d}}, \tag{2.104a}$$

$$S_{21} = \frac{\left(1-\frac{(k_{2x}/k_0-\mu_{2y})^2+\xi^2}{(k_{2x}/k_0+\mu_{2y})^2+\xi^2}\right)e^{\mathrm{i}k_{2x}d}}{1-\frac{(k_{2x}/k_0-\mu_{2y})^2+\xi^2}{(k_{2x}/k_0+\mu_{2y})^2+\xi^2}e^{2\mathrm{i}k_xd}}, \tag{2.104b}$$

where k_{2x} is the wavenumber in the propagation direction inside the medium, governed by the dispersion relation given in Tab. 2.1. In this general case, one cannot define a unique impedance and index of refraction so that the inversion of Eqs. (2.104) needs to be performed numerically as proposed in Chen et al. (2005d). In the special case of a lossless medium, however, Eqs. (2.104) can be simplified as follows:

$$S_{11} = \frac{R_{01}(1-e^{2\mathrm{i}nk_0d})}{1-R_{01}^2e^{2\mathrm{i}nk_0d}}, \tag{2.105a}$$

$$S_{21} = \frac{(1-R_{01}^2)e^{2\mathrm{i}nk_0d}}{1-R_{01}^2e^{2\mathrm{i}nk_0d}}, \tag{2.105b}$$

where $R_{01} = (z-1)/(z+1)$ is the half-space reflection coefficient, and z is the impedance redefined in Tab. 2.1. The inversion of Eqs. (2.105) can then be performed analytically and is straightforward.

The method presented above was first tested on analytical results: assuming a Lorentz model for the permittivity, the permeability, and the bianisotropic term, the reflection and transmission coefficients can be computed and subsequently used in the inversion algorithm. This procedure is therefore a self-check, where the output results are expected to be identical to the input ones, with a total control on all the parameters along the way. The results for both lossless and lossy media are shown in Fig. 2.9 and Fig. 2.10, respectively. In both cases, the method is seen to produce an excellent matching with the reference results, as is expected from an analytical approach.

The next step is to apply the inversion method to the ring of Fig. 2.8, with the reflection and transmission coefficients generated from the forward method shown in Section 2.3. Unlike the reflection and transmission data obtained from an analytical formula as above, those obtained from a numerical code are inherently imperfect and noisy to some extent, very much like those obtained from measurements.

In order to illustrate the necessity of using the bianisotropic retrieval when working with the ring shown in Fig. 2.8, which also highlights the importance of using a correct model when retrieving effective parameters of metamaterials, we first apply the isotropic retrieval of Section 2.4.2 along each direction. With six complex parameters to retrieve (the real and imaginary parts of ε_x, ε_y,

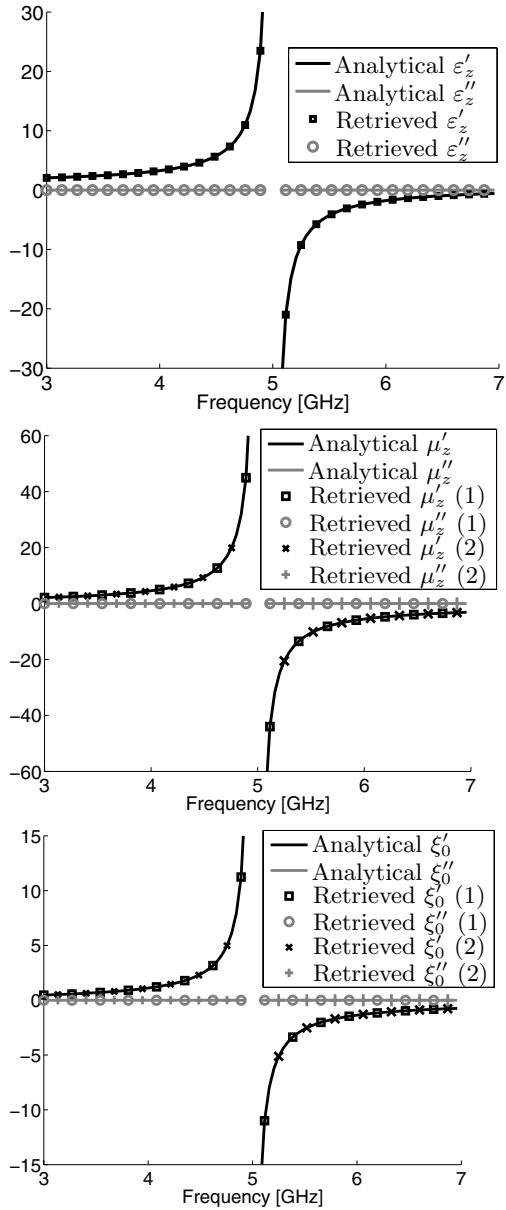

Figure 2.9 Retrieval results on analytical lossless Lorentz models for the permittivity, the permeability, and the bianisotropic term. The matching is seen to be excellent. The results are taken from Chen et al. (2005d; 2006e).

ε_z, μ_x, μ_y, μ_z) and twelve complex sets of data (six incidences that all give a complex reflection and transmission coefficient), we have twice as many equations as unknowns so that each parameter can be retrieved twice, as a consistency check. The results are shown in Fig. 2.11 where two important features are immediately seen: the two values retrieved for ε_x, ε_y, μ_x, and μ_z agree very well all across the frequency range, except for some numerical artefacts due to either noise or resonance of other parameters. However, the two retrieved results for ε_z and μ_y present significant discrepancies, especially close to resonance. These discrepancies prevent us from concluding the correct effective parameter, and illustrate how an incomplete model of a metamaterial may yield inconsistent results.

The bianisotropic study summarized in Tab. 2.1 reveals that the transmission and reflection coefficients involve ε_z, μ_y, and ξ in the incidences TE_2, TM_1, and TM_3 so that it is not surprising to obtain inconsistent results when the bianisotropy is not included. When it is included, however, the results are shown in Fig. 2.12 and reveal a significant improvement in the matching of the two results, giving us confidence that the results as well as the model this time are accurate.

It should now be clear that the inclusion of the bianisotropic term in the model of the split ring shown in Fig. 2.8 is essential. Failure to do so results in biaxial parameters (ε_x, ε_y, ε_z, μ_x, μ_y, μ_z) that are incidence dependent, which is clearly unsatisfactory for a homogeneous medium. This stresses the importance of first developing a correct physical model of the metamaterial under study and then of developing the corresponding inversion algorithm. However, such a model may not always be easy to predetermine, in which case one might try to resort to an all numerical solution without *a priori* assumptions. Needless to say that if no information is known in the tensorial constitutive relation, the problem contains 72 unknowns (nine complex unknowns in four tensors) and is highly nonlinear. The corresponding minimization problem becomes tremendously challenging to solve because of the presence of a very large number of local minima, in addition to requiring heavy computational resources. It is nonetheless interesting to take a closer look at such a method because of its generality.

The minimization problem can be written as follows: :

$$f(\bar{\mathbf{x}}) = \sum_{\phi,\theta} \sum_{i,j\in\{1,2\}} \left\{ |R_{ij}(\theta,\phi) - R^m_{ij}(\theta,\phi)|^2 + |T_{ij}(\theta,\phi) - T^m_{ij}(\theta,\phi)|^2 \right\} , \tag{2.106}$$

where (R_{ij}, T_{ij}) are the reflection and transmission coefficients computed from the method presented in Section 2.3, while (R^m_{ij}, T^m_{ij}) are the measured (and therefore known) reflection and transmission coefficients. The sum over θ and ϕ indicates that multiple incident angles need to be incorporated in order to provide enough equations for the number of unknowns, whereas the sum of (i, j) indicates the two possible incident polarization states. All the

parameters are included in the vector $\bar{\mathbf{x}}$ and the global minimum of f is searched, which corresponds to a relative error between the known parameters and the computed ones smaller than a pre-set threshold. Note that weighting factors are often included in the functional in order to improve convergence, as for example proposed in Chen et al. (2006d).

Essentially two factors influence the choice of the minimization algorithm: the search of the global minimum and the computational time. Deterministic search methods have the advantage of a relatively small computational time but they are very inefficient at searching for the global minimum when too many local minima are present. On the other hand, stochastic methods span the search space more thoroughly but have the disadvantage of being slower. One could therefore think of judiciously combining the two: starting first with a stochastic method (such as a Genetic Algorithm or differential evolution) in order to span the search space and select a few candidates as good initial points for the second stage, where a deterministic method (such as a simplex method) takes over and converges to the minima associated with the initial guesses.

Still, the highly nonlinear optimization problem with 72 parameters might not be solvable and some assumptions might have to be introduced. A reasonable one is that the bianisotropy terms $\bar{\bar{\xi}}$ and $\bar{\bar{\zeta}}$ are zero at low frequencies, thus reducing the number of unknowns by half. The solution obtained in this way can be used as a good initial guess for the retrieval of the first frequency in the recursive algorithm. A second good assumption, which is controllable, is that the material thickness is small, typically less than a wavelength, in order to avoid phase ambiguity. In a broad-band retrieval process, this might require working with two or more sample thicknesses depending on frequency.

With these assumptions, such a parameter retrieval algorithm has been shown to accurately retrieve the frequency dispersive parameters of rotated Omega media (consisting of metallic particles in the shape of Ω) and general bianisotropic media (Chen et al. 2006d). The first example, a rotated Omega medium, is characterized by the constitutive tensors of Eqs. (2.101), to which we add a random rotation along the three Euler angles (α, β, γ). In the $(\hat{x}, \hat{y}, \hat{z})$ coordinate system, the tensors are therefore potentially more complex than simply diagonal, yielding apparently more unknowns than really present in the problem. The various parameters of Eqs. (2.101) have been assumed to take the following analytical forms:

$$\nu_i = 1 - \frac{F_{\nu i} f^2}{f^2 - f_{\nu i}^2 + \mathrm{i}\gamma_{\nu i} f}\,, \tag{2.107}$$

where f is the frequency, $\nu = \{\varepsilon, \mu\}$, $i = \{x, y, z\}$, and where a similar resonance model for ξ has been used with the parameters (F_ξ, f_ξ, γ_ξ). The numerical values of all the parameters are given in Tabs. 2.2. Upon using the differential evolution algorithm at the first stage and two rounds of simplex method at the second stage, the optimized results for all the parameters are

Table 2.2 Parameter definition of Eq. (2.107).

$f_{\nu i}$ [GHz]		i		
		x	y	z
ν	ε	4	5	3.5
	μ	5	4	3.5

$\gamma_{\nu i}$ [GHz]		i		
		x	y	z
ν	ε	0.5	0.4	0.3
	μ	0.4	0.3	0.2

$F_{\nu i}$		i		
		x	y	z
ν	ε	0.5	0.3	0.4
	μ	0.3	0.2	0.3

f_ξ	=	4 GHz
γ_ξ	=	0.5 GHz
F_ξ	=	0.4

α	=	$\pi/5$
β	=	$\pi/4$
γ	=	$\pi/6$

already in good agreement with the expected ones. Fig. 2.13 illustrates the agreement in the bianisotropic term, which is seen to be very good all across the frequency range.

As a second example, we shall mention the parameter retrieval for a general bianisotropic medium which is a chiroferrite medium, as studied in Dmitriev (2001):

$$\bar{\bar{\varepsilon}}_r = \begin{pmatrix} \varepsilon_{xx} & \varepsilon_{xy} & 0 \\ -\varepsilon_{xy} & \varepsilon_{xx} & 0 \\ 0 & 0 & \varepsilon_{zz} \end{pmatrix}, \qquad \bar{\bar{\mu}}_r = \begin{pmatrix} \mu_{xx} & \mu_{xy} & 0 \\ -\mu_{xy} & \mu_{xx} & 0 \\ 0 & 0 & \mu_{zz} \end{pmatrix},$$
$$\bar{\bar{\xi}}_r = \begin{pmatrix} \xi_{xx} & \xi_{xy} & 0 \\ -\xi_{xy} & \xi_{xx} & 0 \\ 0 & 0 & \xi_{zz} \end{pmatrix}, \qquad \bar{\bar{\zeta}}_r = \begin{pmatrix} -\xi_{xx} & -\xi_{xy} & 0 \\ \xi_{xy} & -\xi_{xx} & 0 \\ 0 & 0 & -\xi_{zz} \end{pmatrix}. \tag{2.108}$$

Although some parameters are zero and others are identical to each other, it is important to realize that this information should not be used in a general retrieval, and should in fact come as a result of the method. Like in the previous case, an analytical model can be assumed for all parameters and the retrieval should be carried out in two steps: the first step is run with a stochastic method that explores the entire search space, whereas the second method is run with a deterministic method to converge to a series of solutions. As mentioned previously, successful retrieval results can be obtained in this case when two assumptions are implemented: that the bianisotropic tensors are negligible at small frequency (in fact, only at the first frequency in the frequency sweep algorithm) and that the medium is thin compared to the wavelength. Nevertheless, the encouraging results obtained in Chen et al. (2006d) should merely be viewed as a first step toward a more systematic characterization and retrieval of metamaterials for which a good physical model is yet unknown.

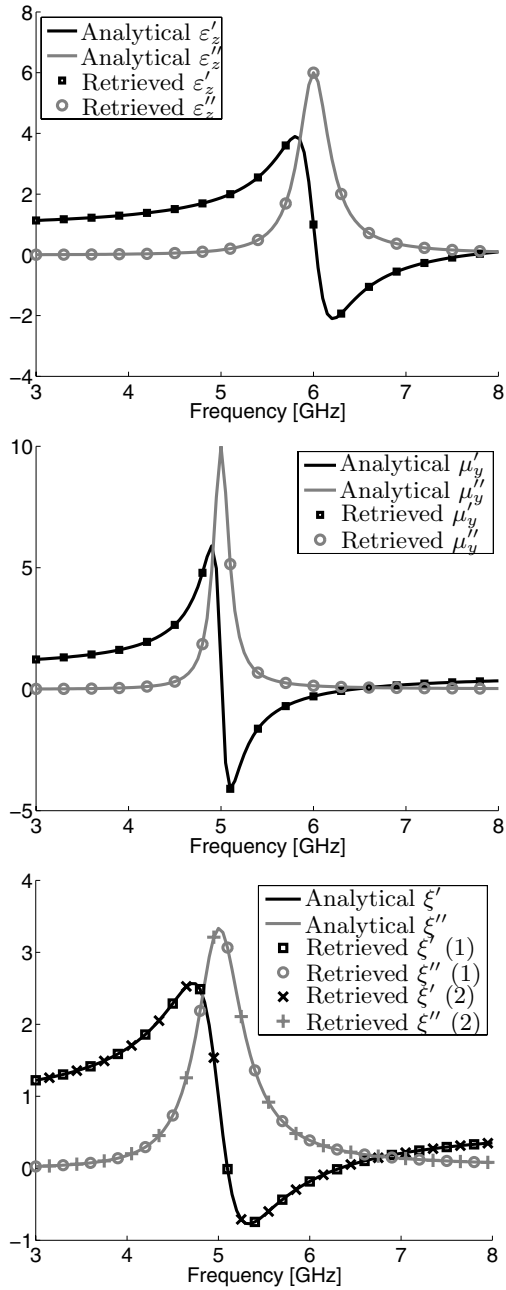

Figure 2.10 Retrieval results on analytical lossy Lorentz models for the permittivity, the permeability, and the bianisotropic term. The matching is seen to be excellent. The results are taken from Chen et al. (2005d; 2006e).

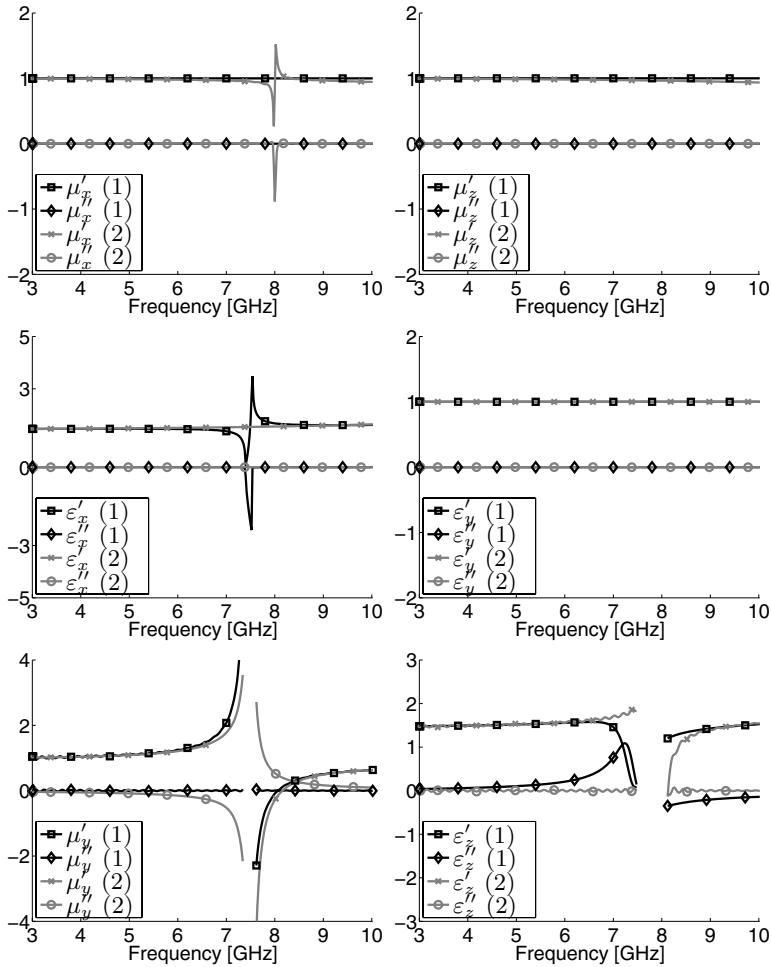

Figure 2.11 Biaxial retrieved parameters of the ring shown in Fig. 2.8 using the method of Section 2.4.2. The blanked regions correspond to frequencies where the mismatch between each corresponding two results is greater than a threshold. The results are taken from Chen et al. (2005d; 2006e).

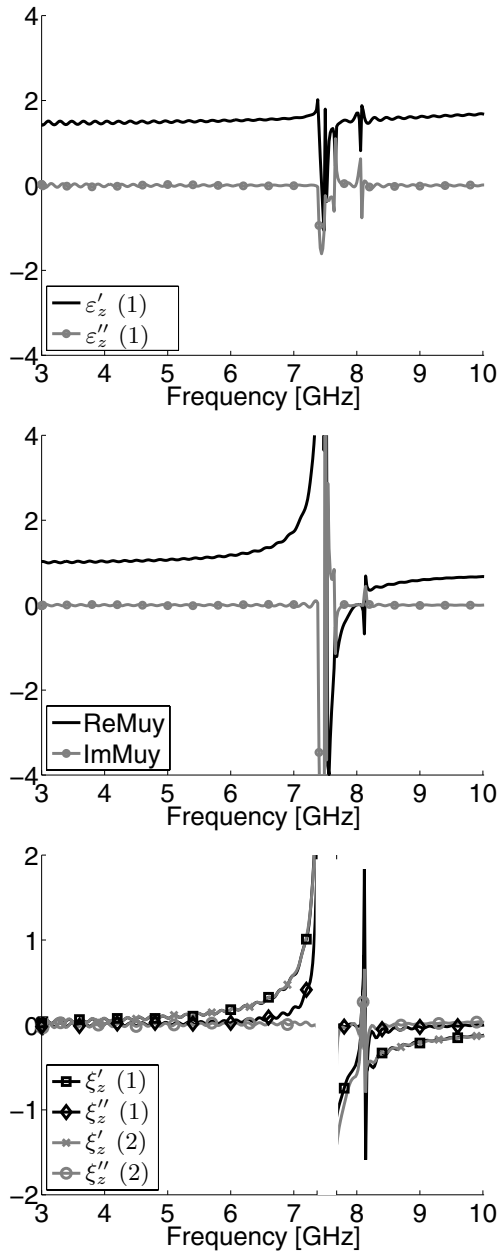

Figure 2.12 Bianisotropic retrieved parameters μ_y, ε_z, and ξ of the ring shown in Fig. 2.8 using the method of the present section. The blanked regions correspond to frequencies where the mismatch between each corresponding two results is greater than a threshold. The results are taken from Chen et al. (2005d; 2006e).

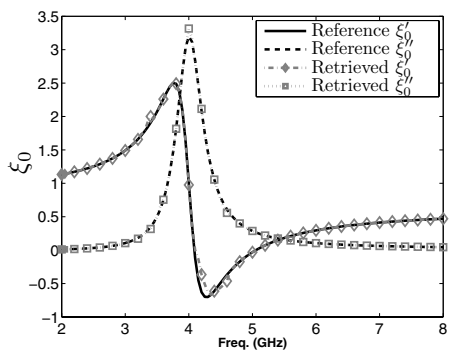

Figure 2.13 Comparison between the retrieved and the forward bianisotropic term of a rotated Omega medium. Results are from Chen et al. (2006d).